Effects of striker compliance on dynamic response and brain tissue strain for helmeted ice hockey impacts

Santiago de Grau Amezcua

Master's thesis dissertation submitted to The Faculty of Graduate and Postdoctoral Studies of the University of Ottawa

In partial fulfillment of the requirements for the degree of
Master of Science in Human Kinetics

Advisor
Thomas B. Hoshizaki, PhD

Committee Members
Gordon Robertson, PhD
Pat Bishop, PhD

School of Human Kinetics
Faculty of Health Sciences
University of Ottawa

Abstract

The effect of striking compliance in ice hockey impacts, and its influence on dynamic response and brain tissue strain was investigated in this study. In hockey, players can experience a broad range of striking/surface compliance during a head impact, from the stiff ice surface to highly compliant player collisions. An increase in striking compliance has been shown to extend the duration of an impact that is associated with an increase in risk of sustaining brain injuries. Three striking caps of low, medium, and high compliance were used to impact a helmeted 50th percentile Hybrid III male headform attached to an unbiased neckform. Each level of compliance was used to impact five high risk locations at three different velocities, representative of head impact scenarios in ice hockey. The dependent variables, peak resultant linear accelerations and peak resultant rotational acceleration as well as MPS, were analyzed using a multivariate analysis of variance (MANOVA) to determine if there were significant differences between the three controlled variables. The results demonstrate a significant effect of compliance, over the influence of velocity and acceleration. Conditions of low impact compliance resulted in higher response values compared to impacts of increased compliance. That being said, high compliance conditions remained in the range of concussion risk, even at the lowest velocity. The use of brain tissue modeling, compared to dynamic response alone, demonstrated an elevated risk of brain injury as a result of extended impact durations. Impact compliance in hockey is a factor that has not been considered when designing and testing helmet technology. The results of this study demonstrate that compliance is a determining factor in producing brain injury, and should be incorporated into helmet standard testing to mitigate risk. The results of this study have implications on brain injury risk that extend beyond

the impacting scenarios of ice hockey. The results can be extrapolated to any contact sport that includes impacting scenarios against varied impacting compliances such as football and rugby.

Acknowledgments

Thank you to the team at NISL for your help during the challenges of writing my thesis, and making my time in the lab a great and memorable experience. It was a pleasure working with you all and I wish you the best.

It has been a privilege to work with Dr. Blaine Hoshizaki during my undergraduate and graduate studies. I am very grateful for everything that I have learned, you're an outstanding researcher and exceptional leader. Thank you for your guidance and standard of excellence which continuously pushed me to work hard and improve myself. And special thanks to Andrew Post as well for being a great mentor during my time in the lab.

Thank you to my committee members Dr. Gord Robertson and Dr. Pat Bishop for evaluating my thesis and providing feedback. Your perspective and expertise was valuable in improving my work. I appreciate your time.

Most importantly I want to thank my parents, sister, and especially Krista Campbell for your love and support during the difficult moments that this degree presented. I will always be grateful.

List of Tables

List of Figures

(medium compliance) and green is 20 + ms (high compliance). Red lines represent traumatic brain injury risk.

Fig 16. Peak MPS response for the three levels of compliance across the five impact locations at a striking velocity of 7.5 m/s. 50% injury risk is shown by the dashed lines and their respective studies. Risk duration is matched to the condition where orange is 10-20 ms (medium compliance) and green is 20 + ms (high compliance). Red lines represent traumatic brain injury risk.

Fig 17. Acceleration time graphs which demonstrate examples of a short duration impact (left: high velocity, side, low compliance) and a long duration impact (right: low velocity, side, high compliance).

Table of Contents

Chapter 1

1.1 Introduction & Statement of Problem

Worldwide, it is estimated that 1.6-3.8 million sport related brain injuries occur each year (Collins et al., 2003; Langlois et al., 2006). These injuries lead to long term health deficits and have a large social and economic burden on society, with an estimated annual cost of $ 3 Billion in Canada alone (The Brian Association, 2007). The most common injuries are mild traumatic brain injury (mTBI), also known as concussion (Mori et al., 2006). Ice hockey has been identified as having the highest rate of concussion per participant in the sporting world (Koh, Cassidy, & Watkinson, 2003). It is also the sport with the highest number of concussions in Canada, accounting for up to 18% of all hockey injuries (Tator, 2009; Emery et al. 2006). The use of certified hockey helmets (CSA Z262.2-M90) has resulted in the near elimination of skull fracture and traumatic brain injuries (TBI), though concussions have not been managed as successfully (Wenneberg & Tator, 2003; Hoshizaki & Brien, 2004). This may be the result of how helmets are evaluated, with a standard method that replicates the mechanisms of focal injuries such as TBI and skull fracture, by dropping the head onto a rigid surface. Research has reported that mechanisms of concussion may be the result of the head impacting a softer and more compliant surface (Willinger et al., 1994; Kleiven, 2005; Gilchrist, 2003; Rousseau, 2004). As there are a variety of compliant impact surfaces in ice hockey, beyond the falling to ice that is simulated in the standard, it is important to investigate how ice hockey helmets perform under these different conditions.

For a helmet to effectively protect against concussion, the mechanisms of injury in hockey must be understood. Studies on concussive injuries in elite level hockey have reported

falls to ice only account for 7% of concussion cases (Hutchinson et al., 2015a, 2015b). In head impact biomechanics, falls have been characterized by the mass of the head impacting a stationary rigid surface resulting in high magnitude and short duration acceleration-time curves (Hoshizaki et al., 2014; Post et al., 2012; 2014). Player-to-player collisions account for 88% of events resulting in concussion, with shoulder-to-head impacts being the most common mechanism of injury (Hutchinson et al., 2015a, 2015b). Player collisions are characterized by low magnitude and long duration events, as the energy of the collision is redistributed and elongated due to an increase in striking compliance (Rousseau, 2014). These extended event durations have been linked to an increased risk of sustaining diffuse brain injuries including concussion (Gurdjian et al., 1953, 1954, 1966; Gennarelli, 1983; Willinger et al., 1992; Gilchrist, 2003; Kleiven, 2005; Rousseau, 2014). This could explain the ongoing high incidence of concussive injuries in ice hockey as helmets are designed and tested to only protect within a narrow window of low striking compliance. The focus of this study was to investigate the influence of striking compliance on dynamic and brain tissue response.

1.2 Background & Significance

The effect of striking compliance during hockey impacts has not been previously considered in helmet performance and design, even though it plays a key role in the mechanisms of brain trauma. It is important that improvements are made in helmet performance in consideration of the reported long term effects of concussion on health and well-being of participants (Daneshvar et al., 2011).

Chronic Traumatic Encephalopathy (CTE) is a progressive neurodegenerative disease believed to be the result of repetitive brain trauma from multiple concussions during an

athletes career (Tartaglia et al., 2014). CTE diagnosed in retired athletes has attracted a great deal of attention in the past decade as they continuously struggle with symptoms including irritability, anxiety, emotional lability, depression, substance abuse, and in some cases suicide or homicide (Brainard et al., 2012; Tator, 2009). Considering the inherent limitations associated with present helmet standard testing, the goal of this paper was to develop a test to reflect helmet performance in reducing the incidence of concussion for compliant impacts. This involves modifying the level of impactor compliance to reflect what is most often experienced during concussive impacts in hockey.

Compliance is defined as the rigidity of an object and the extent to which it resists or deforms in response to an applied force (Baumgart, 2000). An increase in compliance results in greater elasticity of an impact, elongating the duration at which the two (or more) objects are in contact with each other, and as a consequence the amount of time that the two bodies are subjected to the force resulting from the collision. It has been proposed that low compliance impacts with long event durations (over 15 ms) can be considered safe as far as cerebral concussion is concerned (Hodgson & Thomas, 1972). This supports the notion that helmets should be designed to protect against low compliance impacts. There is also a large amount of research that contradicts this theory, as it has been reported that the duration of the event does have an influence on brain injury and risk of concussion (Gurdjian et al., 1953, 1954, 1966; Gennarelli, 1983; Willinger et al., 1992; Kleiven, 2005; Gilchrist, 2003). During a collision in ice hockey, impact compliance is increased as a result of protective padding and helmets, as well as the natural movements of the human body which manage and redistribute energy through joints and muscles. Rousseau (2014) reconstructed real world concussive impacts in hockey to

investigate event durations for different mechanisms of brain injury. Collisions with an opponent resulted in peak acceleration/time curve durations of 20-30 ms which characterized a long duration head impact event in ice hockey. Collisions in hockey are composed of impacts against a padded surface of the body, such as the shoulder which is the most frequent point of contact to the head during collisions (Rousseau, 2014). Padding, and helmets attenuate the magnitude of an event but result in extended durations of head acceleration. Short event durations that range between 5-10 ms represent impacts against low compliance surfaces, such as when a player strikes his head on the ice. An unyielding surface will transfer the majority of the energy of an impact to the head, resulting in an inelastic collision and short duration event. Finally, collisions against harder and less padded surfaces on the body, such as an elbow, are represented in impacts ranging between 10-20 ms.

The first studies to report the relationship of extended loading durations to the brain and increased risk of injury to the tissue involved animal research. They demonstrated that low magnitudes of acceleration can cause diffuse axonal injuries (DAI) if the duration of the impact is elongated (Gurdjian et al., 1953, 1954, 1966; Gennarelli, 1983). High magnitude accelerations from a short duration event can cause concussion but are more closely associated to TBI such as hematoma at different levels of the brain tissue (Gurdjian et al., 1953, 1954, 1966; Gennarelli, 1983). Studies employing finite element modeling have demonstrated that long duration events are associated with diffuse brain injuries as a result of shear forces in the brain tissue leading to intracerebral stresses and strains producing widespread hemorrhagic lesions (Willinger et al., 1992; Kleiven, 2005; Gilchrist, 2003). The results of this study build upon this

knowledge and can be used to evaluate and compare the effects of compliance and event duration on different mechanisms of injury in hockey.

1.3 Research Question

What is the effect of striker compliance on dynamic response and brain tissue strain on a helmeted Hybrid III headform, for different levels of velocity chosen to replicate on ice collisions?

1.4 Objectives

The objective of this study was to evaluate the magnitude and duration of dynamic response of the head and brain tissue strain at different levels of striking compliance. The impact sites chosen represent high risk locations for sustaining concussion on a human head. Furthermore, the impact velocity was set to reflect commonly observed collision speeds in the sport which lead to concussive injuries. Evaluating the effect of compliance provides a better understanding of the mechanisms of concussion during player collisions in ice hockey, as well as describes the protective capacity of current hockey helmet technology.

1.5 Variables

1.5.1 Independent Variables (3x3x5)

1. Compliance: (3 levels) Low compliance, Medium compliance, High compliance
2. Velocity: (3 levels) Low (4.5 m/s), Medium (6.0 m/s) and High (7.5 m/s)
3. Location and impact vector (5 levels) (uOTP[5])

1.5.2 Dependent Variables

1. Dynamic Response:
    a. Peak Resultant Linear Acceleration of the headform (g)

b. Peak Resultant Rotational Acceleration of the headform (rad/sec^2)

2. Brain tissue measures: Maximum principal strain of the brain (MPS)

1.6 Experimental Hypothesis

1. It was hypothesized that increasing striking compliance would decrease peak linear acceleration of the Hybrid III headform (g).
2. It was hypothesized that increasing striking compliance would decrease peak rotational acceleration of the Hybrid III headform (rad/s^2).
3. It was hypothesized that increasing striking compliance would increase brain tissue response (Maximum principle strain).
4. It was hypothesized that increasing velocity would increase the peak linear acceleration of the Hybrid III headform (g).
5. It was hypothesized that increasing velocity would increase the peak rotational acceleration of the Hybrid III headform (rad/s^2).
6. It was hypothesized that increasing velocity would increase the brain tissue response (Maximum principle strain).
7. It was hypothesized that non-centric impact locations would decrease the peak linear acceleration of the Hybrid III headform (g).
8. It was hypothesized that non-centric impact locations would increase the peak rotational acceleration of the Hybrid III headform (rad/s^2).
9. It was hypothesized that non-centric impact locations would increase the brain tissue response (Maximum principle strain).

1.7 Limitations

1.7.1 Hybrid III headform

The 50th percentile Hybrid III headform acts as a surrogate of the human head during reconstructive testing. The Hybrid III headform was designed by Hubbard and McLeod (1974) as part of a GM project in order to develop an anthropometric test device which can serve as a human surrogate for car crash accidents. The headform was designed to produce data which are within the ranges found for cadaveric head drop studies and be able to sustain multiple high impacts without breaking. The material characteristics of the headform, steel covered by an unattached vinyl cover, increases weight and rigidity and as a result it responds differently under loading conditions compared to a real human head, limiting its biofidelity. The assumption made for this experiment was that the Hybrid III headform responds as a human head would to predict brain injury risk.

1.7.2 UCDBTM

Brain tissue response is dependent on the material properties assigned to it. There are variations in the literature on material properties of the head/brain making it difficult to establish a global value for these properties. UCDBTM's material properties are taken from multiple studies (Ruan, 1994; Willinger et al., 1995; Zhou et al., 1995; Kleiven and von Holst, 2002) which allows the response of the model to be within reasonable bounds of true response. The assumption made for this experiment was that the MPS of the brain are representative of strain response of live humans.

1.7.3 Multiple levels of compliance

There are multiple contributing levels of compliance for impacts in this study. For example, helmets increase the compliance of an impact through their protective lining, which results in lowering the magnitude of force during a hit to the head. Also, the skin-form on the Hybrid III headform contributes to impact compliance due to is soft material makeup which covers the rigid steel frame of the head. That being said, these factors remained constant for all conditions and therefore observed changes are the result of the striking cap compliance.

1.7.4 Evaluating brain injury risk

It is important to note that injury risk values from the literature were obtained using different impacting parameters than the ones in this study. The assumption was made that the injury risk values for dynamic response and MPS included in this study reflect concussion risk in ice hockey.

1.7.5 Striking Caps

The Striking caps represent were developed to represent the different levels of striking compliance observed in ice hockey. The assumptions were made that the high and medium compliance caps are reflect on ice player collisions, and the low compliance striking cap reflects a fall to ice.

1.7.6 Helmet

A single model of a certified ice hockey helmet, Reebok 11k VN Medium, was used for this study and therefore the assumption was made that all hockey helmets respond in a similar fashion.

1.8 Delimitations

1.8.1 Impact velocity

There are wide ranges of impacting velocities that occur during concussive impacts in hockey (Rousseau, 2014). The impacting velocities for this study are delimited to match standard testing, up to the average impacting velocity of shoulder impacts reported by Rousseau (2014; NISL, 2014).

1.8.2 Impact location and angle

Although hockey players are at risk of being hit anywhere on the head and face, the impact locations for this study were delimited to the five impact conditions that represent an 80% risk of sustaining a concussion (Walsh et al., 2011).

1.8.3 Unbiased neckform

The commonly used Hybrid III neckform was developed for inertial loading in the sagittal plane and may impart unnatural bias to the motions out of this plane (Walsh & Hoshizaki, 2012). Therefore an unbiased neckform was used for this study.

1.8.4 Striking mass

The striking mass remained constant for this experiment for all striking conditions. The assumption was made that the striking mass is representative of on-ice player collisions and falls to ice for all striking velocities.

Chapter 2

2.1 Literature Review

2.1.1 Introduction

A concussion is defined by the American Academy of Neurology as trauma induced alteration in mental status that may or may not involve the loss of consciousness. Concussions have been described as diffuse injuries resulting from microscopic tears in the white matter/axons without visible damage to the cortex (Strich, 1961). Athletes are at risk of sustaining concussions which have been linked to long term health deficits such as CTE, and are also believed to play a role in initiating and accelerating the molecular cascade involved in other neurodegenerative diseases including Alzheimer's, Parkinson, and ALS (Daneshvar et al., 2011). Therefore the incidence of concussions must be mitigated in sport. Concussion risk can be estimated experimentally by reconstructing impacts under laboratory conditions using physical, mathematical, and computational models (Post & Hoshizaki, 2012). Traditionally, cadaver and animal models have been used to study the mechanisms of injury to the brain tissue (Gurdjian et al., 1953, 1954, 1966; Hodgson et al., 1966; Gennarelli et al., 1971, 1972; Nahum et al., 1977; Hardy et al., 1997; Hardy et al., 2001). The primary advantage of cadaveric test studies is that they have the same geometry and mass distribution as a living human (Gilchrist et al., 2001). Unfortunately, due to the pathophysiological differences of the living to cadaveric brains, the information the results of these studies provide might not fully represent the mechanism of injury in living tissue. Animal testing provides living models that can be used to investigate living brain tissue response, though limitations arise in the extrapolation of the data due to anatomical and physiological differences (Xiong et al., 2013).

Injury reconstruction using dummies is a common method in brain injury research as it provides valuable information on the mechanisms of concussion, with possible extrapolation to the general population (Zhang et al., 2004). Headforms instrumented with an internal accelerometer array can measure both linear and rotational accelerations of the head during a reconstructive impact. The output, or dynamic response, can be analyzed using established injury risk values and computer models. The following sections examine dynamic response and brain tissue variables, as well as the effects of compliance on brain injury risk.

2.1.2 Dynamic Response

Linear acceleration has been used as a performance metric during helmet testing based on research identifying a correlation between it and intracranial pressure (ICP) (Gurdjian et al. 1966; Thomas et al., 1966). Research using animal and cadaver models has shown that linear impacts cause brain deformations associated with raised ICP, that lead to focal injuries in the brain (Haddad et al., 1955; Gurdjian et al., 1966; Thomas et al., 1966; Unterharnsheidt & Higgins, 1969). The inertia of the brain pushing up against the impact site as it lags behind the faster moving skull creates an area of high pressure known as the coup injury site. Furthermore, at the distal/contrecoup site, this translation of the brain within the skull creates corresponding areas of negative pressure that can also cause damage to the tissue (Gurdjian & Gurdjian, 1975). The use of linear acceleration as an injury metric has been successful to date, resulting in the reduction of focal injuries such as skull fracture and TBI, but it has not however reduced the incidence of diffuse injuries like concussion (Wenneberg & Tator, 2003).

The use of linear acceleration is not fully descriptive of all brain injuries, including concussions that have been associated to rotational accelerations. Holbourn (1943) first

proposed the theory that rotations of the head are the primary cause of brain injury. Using a physical model he described how the stresses and strains in the brain were primarily influenced by rotational motion. Injury was the result of the inability of the brain to rotate within the skull that causes strains to the brain tissue. The brain's high bulk modulus and low shear modulus makes shear-stress a more likely mechanism of injury. Considering that shear-stress and rotational acceleration are correlated, it was concluded that rotational acceleration was responsible for concussion and hemorrhages (Holbourn, 1943). Using primates, Gurdjian et al. (1968) investigated the theory that injury evoked by rotational dynamics is the result of diffuse shearing of brain tissue. It was concluded that injurious strains developed in the brain as a result of difference in tissue material properties and the transmission of forces through them. Further investigation of this phenomenon has shown to cause focal and diffuse injuries (Ommaya & Gennarelli, 1974; Yoganadan et al., 2008). Non-impact, pure rotational accelerations using primates revealed subdural hematoma, torn bridging veins, and brain lesions can occur as a result of rotation alone (Unterharnsheidt & Higgins, 1969). Non-contact linear accelerations do not produce concussive injuries (Gennarelli et al., 1971, 1972). These findings have been further supported by Hardy et al. (1994), as they demonstrated that the inability of the brain to rotate within the skull causes focal point shear stresses and strains. Kleiven (2006) found that rotational acceleration has a high correlation with peak strains. Forero Rueda et al. (2010) also found that rotational acceleration was correlated with stress and strain in brain tissue while linear acceleration had a lower correlation. In summary, rotational dynamics was incorporated in concussion testing as the shear stress and strain produced by these accelerations is associated with the injury. Furthermore, dynamic response

is a valuable tool to measure the magnitude and duration of linear and rotational accelerations that the brain is subjected to during reconstructed events. The effect of compliance on dynamic response is outlined in the following sections.

2.1.3 Finite Element Analysis

Improvements in computer modeling have allowed for the use of finite element (FE) analysis as a tool to measure the risk for brain injuries. FE modeling has been widely used as a numerical surrogate to simulate head mechanical responses under a variety of impact and inertial conditions (Zhang et al., 2001; King et al., 2003; Forero Rueda et al., 2010). FE analysis is an important tool when evaluating head dynamic response as it allows for the interpretation of linear and rotational acceleration curves and their influence on brain injury. Brain material characteristics and how they respond to an impact scenario influences the severity of tissue damage in the brain (Prange et al., 2002). It has been documented that the material properties of the brain have different characteristics and anisotropic in nature. Being composed of different types of tissue, the brain deforms in an inhomogeneous manner creating shear stress and strains that in turn cause lesions in brain matter (Strich, 1961). FE models measure brain deformation of an impact through the three linear components and three rotational components of acceleration over time for a full representation of the event. This allows for the inclusion of direction and magnitude, as well as other loading curve characteristics that influence brain deformation (Post et al., 2012). The brain tissue deformation value used in this thesis was maximal principle strain (MPS) which represents the highest strain value along the three principle axis (x, y, z). MPS was chosen as a predictor of brain injury as it has shown to correlate with diffuse axonal injuries (Bain & Meaney, 2000; Bain et al., 1997; Galbraith et al.,

1993; Thibault, 1990; Gennarelli et al., 1989), and has also been identified as a predictor for concussion (Zhang et al., 2004; Kleiven, 2002; Willinger & Baumgartner, 2003; Zhou et al., 1995). In summary, finite element modeling allows for the interpretation of dynamic response loading curves, and how different factors such as striking compliance contribute to injury risk and location. The incorporation of FE analysis during helmet testing could provide insight into how helmets protect athletes during different impacting conditions, including striking compliance.

2.1.4 Evaluating injury risk

Employing simulations and reconstructions, injury risk can be established using variables such as dynamic response and brain tissue strain. These proposed percent injury risk values can be useful in evaluating impact outcomes; however it is important to account for the different methodologies used to obtain these values. Proposed mechanisms of brain trauma have one common variable; a certain amount of measureable deformation stresses the brain tissue resulting in permanent deformation and injury (Post & Hoshizaki, 2012). Identifying levels of brain tissue deformation with injury risk may provide a useful method interpreting outcome variables of a head impact. Establishing a universal threshold is difficult though as there are many variables that contribute to the level of injury risk, such as anatomical and physiological differences of the person and variability of impact mechanisms. Few studies have taken into account the impact duration when establishing injury thresholds in sporting events.

Zhang et al. (2004) reconstructed American football impacts based on video footage of real world collisions. Twenty-four helmet-to helmet field collisions were reconstructed and analyzed using an FE model. The results of this study provided percent injury risk values that are

widely used today when evaluating kinematic response. Zhang et al. (2004) estimated that the peak resultant linear acceleration of the head was 66, 82, and 106 g for a 25%, 50%, and 80% probability of concussion, respectively. Furthermore, the maximum resultant rotational accelerations for a 25%, 50%, and 80% probability of sustaining concussion were estimated to be 4.63, 5.93, and 7.93 krad/s^2 respectively. These values represent impact durations between 10ms to 30ms.

McIntosh (2014) and Patton (2015) both derived their injury risk values from the same database of impacts in adult male professional Australian Rules football. McIntosh's study presents human tolerance estimates for concussion based on linear and rotational accelerations of the head using computer reconstructions of rigid body simulations. The results of the study determined a 50% and 75% likelihood of concussion for resultant linear head acceleration values of 65.1 and 88.5 g, respectively. Rotational tolerance values of 1,747 rad/s^2 and 2,296 rad/s^2 were reported for a 50% and 75% likelihood of concussion, respectively. Patton (2015) used a detailed finite element model of the human head to approximate the regional distribution of tissue deformations in the brain from the simulated impact reconstructions of Australian rules football. The results were evaluated using logistic regression analysis and it was found that MPS, in all regions of the brain, were significantly associated with concussion. Strain tolerance values of 0.13, 0.15, and 0.26 in the thalamus, corpus callosum, and white matter, respectively, resulted in a 50% likelihood of concussion (Patton et al., 2015). McAllister et al. (2012) used on-field monitoring in football and ice hockey using instrumented helmets to record head impacts sustained during play. He combined this data with finite element (FE) biomechanical simulation, allowing for predictions of regional strain associated

with a diagnosed concussion. The results of his study proposed peak resultant linear and rotational head accelerations of 73.6 g and 5025 rad/s^2 as injury risk tolerance values for concussion.

Rousseau (2014) provided tolerance values for concussion in 27 elite hockey reconstructed concussive and no-injury impacts. As previously mentioned, the study found that concussive impacts had longer mean duration times compared to non-injurious impacts of the same mechanism. A binary logistic regression analysis was used to evaluate the effects of linear and rotational acceleration curve durations on the likelihood of sustaining a concussion. The author established a 50% likelihood of concussion for a peak rotational acceleration of 9.2, 6.9, 4.6, and 2.2 krad/s^2 for peak acceleration/time curve durations of 15, 20, 25, and 30 ms, respectively. Furthermore, a 50% likelihood of concussion was established for a peak linear acceleration of 23, 15, and 7 g for peak acceleration/time curve durations of 15, 20, and 25 ms, respectively. As the acceleration pulse duration was extended, the magnitude of acceleration needed to cause injury decreased.

Finite element modeling has been used to establish injury risk using brain tissue response values. Zhang et al. (2004) established strain tolerance values of 0.14, 0.19, and 0.24 for 25%, 50%, and 80% chance of concussion, respectively. Kleiven (2007) has also investigated tolerance values of injury using a validated FE model (Kleiven & Hardy, 2002). The results of the simulation indicated a 50% probability of concussion for MPS with a value of 0.21 in the corpus callosum and 0.26 in the grey matter (Kleiven, 2007). The differences in concussive tolerance values in the literature for both dynamic response and FEA are the result of case selection, impact parameters inherent to each sport, and methodology used. In summary, percent risk of

injury tolerance values are an important tool when analyzing reconstructed data as they allow for interpretation of the degree of severity of an impact and its components.

2.1.5 Compliance and mechanisms of injury

Gurdjian et al. (1953) investigated the effect of impact duration on the risk of concussion in canines using a pressure driven piston to hit the head. Their results demonstrated that event duration was the single significant factor that explained the clinical effects following a concussive impact, when compared to head acceleration and applied piston pressure. It was noted that low magnitudes of acceleration can cause concussion if the duration of the impact is elongated, while high magnitude accelerations can cause concussion from a short duration event. A follow-up study by the authors found similar results in that the longer the duration of an impact, the lower the required magnitude of force needed to produce a concussion (Gurdjian et al., 1954). Using animal and cadaver data, an acceleration-time tolerance curve known as the Wayne State Tolerance Curve (WSTC, Fig. 1) was developed by Gurdjian et al. (1966). What this curve exemplifies is that high linear accelerations can be tolerated for short durations while lower accelerations can be tolerated for longer durations, summarizing their previous research. This relationship was also confirmed by Ono et al. (1980), who developed the Japan head tolerance curve.

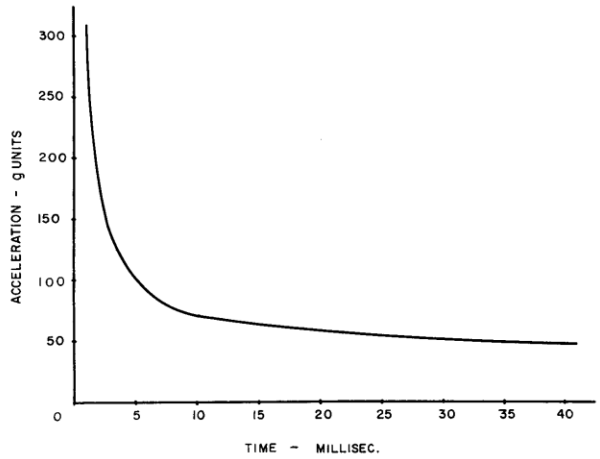

Fig 1. Wayne State Tolerance Curve for the human head acceleration in gravity units, time in milliseconds.

The mechanisms of focal and diffuse injuries to the brain were investigated by Gennarelli (1983) using post mortem human and live animal models. He found that SDH is caused by short duration loading at high rates of acceleration. In SDH the primary damage occurs to surface blood vessels. These circumstances occurred as a result of falls, where the head rapidly decelerates from an impact to a firm and unyielding surface. DAI was caused by longer duration, lower magnitude rotational accelerations of the head upon impact to a deformable or padded surface. This resulted in a lengthening of the deceleration rate (Gennarelli, 1983). In DAI, the principle mechanical damage is to the brains axons, similar to what would be observed during a concussive injury. Directional loading was also investigated as the author found that side impacts caused acceleration in the coronal plane and lead to the highest severity of injury to the brain (Gennarelli, 1983).

Using mathematical modeling and epidemiological data from post mortem cases, Willinger et al. (1992) investigated the relationship between injury distributions and different impacting stiffness at lateral and occipital impact sites. They proposed that there is a change in the injury mechanism that occurs as a function of event duration. During short duration impacts

on medium to low compliance surfaces, there is relative motion between the brain and skull with the consequent potential for injury. The brain becomes decoupled from the skull and moves independently causing damage from direct contact with the skull (Willinger et al., 1992). This mechanism may be responsible for most peripheral injuries such as acute subdural hemorrhaging caused from the rupture of veins bridging the gap between the brain and the skull. For impacts with striking surfaces of high compliance, the brain tends to move with the skull. These movements result in intracerebral stresses and strains that produce hemorrhagic lesions in the central parts of the brain and spread out through the cortex. The results revealed that long duration impacts lasting between 15 ms to 20 ms resulted in diffuse brain injuries. It was also reported that the dominant injuries associated with short peak acceleration pulse durations are caused by linear translations of the head, while injuries with longer peak acceleration pulse durations are associated with the rotation of the head (Willinger et al., 1992).

With the advancements in computer technology, brain models have allowed for a detailed analysis of the mechanisms of brain injuries. Kleiven (2005) analyzed the effects of different load directions and durations following an impact using a detailed finite element model of the human head. Using rotational acceleration the author found that an increase in the strain level of the brain tissue was obtained from an increase in the peak acceleration pulse duration of an impact to the head. It was also reported that loading in the lateral direction was more likely to cause diffuse brain injuries compared to loading in the sagittal plane (Kleiven, 2005). In summary, there was an inverse relationship between the magnitude of an event and its duration when compliance is modified. The aforementioned studies provide evidence to

support the notion that impacts with high compliance surfaces induce extended durations of lower magnitudes that can increase the risk of sustaining brain injury, including concussion.

2.1.6 Summary

Research investigating the effects of striking compliance demonstrated that as duration of the impact increased there was an increase in the risk of sustaining concussive injuries. Current helmet testing certification is designed to primarily replicate the injury mechanism associated with TBI and skull fracture. As a result, such injuries are very rare in ice hockey. Concussion however remains common in ice hockey suggesting that a different mechanism of injury. Compliance may be a factor in the mechanisms of concussion in ice hockey as the aforementioned studies have associated extended loading of the brain tissue, that is a result of increased compliance due to the existence of padding in the sport, to diffuse injuries like concussion. The objective of this study was to further the understanding of the effects that striking compliance on the risk of concussion in ice hockey.

Chapter 3

3.1 Methodology

Three striking caps of low, medium, and high compliance were used to impact the head. Each level of compliance was used to impact five high risk locations at three different velocities. A helmeted 50th percentile Hybrid III male headform attached to an unbiased neckform was used to assess the effect of striking compliance during an impact. Peak linear accelerations were measured using a "3-2-2-2" array of accelerometers mounted inside the Hybrid III headform and rotational accelerations were calculated to describe the dynamic impact response (Padgaonkar et al., 1975). The dynamic response from the impacts was used as input

into the University College Dublin Brain Trauma Mode (UCDBTM) to determine MPS within the brain tissue.

3.1.1 Equipment

A pneumatic linear impactor (Fig. 2) was used to strike the headform. It consists of a stationary steel frame secured to a cement floor. The frame supports a cylindrical free moving impactor arm (length 1.28 ± 0.01 m; mass 16.6 ± 0.1 kg). Following an electronic trigger, a pneumatic propulsion arm system attached to the posterior part of the frame accelerates the impactor arm to striking velocity. Subsequent to this acceleration phase, the impactor arm disconnects from the propulsion arm and is under no influence from external forces travelling at target speed until impacting the headform. Velocity of the impactor arm was controlled by changing the amount of pressure in the system through a manual valve. An increase of Pascals (Pa) in the pressure tank results in higher acceleration of the arm. Inbound velocity was measured immediately prior to impact using an electronic time gate (width 0.2525 ± 0.0001 m) and recorded by a computer.

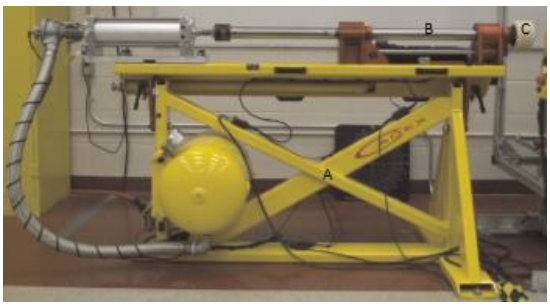

Fig 2. Pneumatic linear impactor frame (A) and impacting arm (B) and striking cap (C).

A 50th-percentile adult male Hybrid III headform (mass 4.54 ± 0.01 kg) was used for all impacting conditions. The Hybrid III headform was based on cadaveric data and was designed to respond to an impact similarly to how the human head would (Yoganandan et al., 2009).

Nine calibrated single-axis Endevco 7264C-2KTZ-2-300 accelerometers are fixed inside the headform according to Padgaonkar's orthogonal 3-2-2-2 linear accelerometer array developed to measure and calculate three-dimensional motion during an impact (Padgaonkar et al., 1975). The following equations were used to calculate the rotational acceleration based on the first principles of rigid body dynamics and linear acceleration from the orthogonally arranged sensor array.

$$\overrightarrow{\alpha_x} = \frac{\overrightarrow{a_{zS}} - \overrightarrow{a_{zC}}}{2S} - \frac{\overrightarrow{\alpha_{yT}} - \overrightarrow{a_{yC}}}{2T} \qquad [1]$$

$$\overrightarrow{\alpha_y} = \frac{\overrightarrow{a_{xT}} - \overrightarrow{a_{xC}}}{2T} - \frac{\overrightarrow{\alpha_{zF}} - \overrightarrow{a_{zC}}}{2F} \qquad [2]$$

$$\overrightarrow{\alpha_z} = \frac{\overrightarrow{a_{yF}} - \overrightarrow{a_{yC}}}{2F} - \frac{\overrightarrow{\alpha_{xS}} - \overrightarrow{a_{xC}}}{2S} \qquad [3]$$

Where α_i is the rotational acceleration for component i (x, y, z) and α_{ij} is the linear acceleration for component i (x, y, z) along the orthogonal arm j (S, T, F) (Padgaonkar et al., 1975). The headform coordinate system was defined with a left-hand rule and positive axes directed anteriorly, toward the right ear and caudally for x, y and z respectively (Walsh et al., 2011). The accelerometers were sampled at 20 kHz and filtered using the SAE J211 class protocol. The accelerometer signals are passed through TDAS Pro Lab system before being processed by TDAS software.

The Hybrid III neckform was designed and validated for impacts in the anterior/posterior direction and it is unknown how this directional bias influences the dynamic impact response of a headform. The unbiased neckform (Fig. 3) was created to match the mass and dimensions of the Hybrid III neckform with four centred and unarticulated rubber butyl disks (radius 68.0 mm and height 21.5 mm) recessed slightly and serially inside aluminium disks (85.6 mm in radius

and 12.8 mm in height) (Walsh & Hoshizaki, 2012).The tension of the neck was matched to that of the Hybrid III neckform at 1.10 Nm. This was achieved using a torque wrench and tightening the wire to the appropriate torque measurement. The unbiased neckform has been designed to respond the same to impacts in all directions and therefore eliminate any potential biased effects of the Hybrid III neckform (Walsh & Hoshizaki, 2012).

Fig 3. Unbiased neckform used in this study, front view.

The Hybrid III head and unbiased neckform were connected to a sliding table base (mass 12.78 ± 0.01 kg) and linear rail system through a locking device adjustable linearly in all three axis and rotationally in the y- and z-axis using a locking device. This enables the researcher to control the location of impact as the impacting arm cannot be moved. The linear rails were aligned longitudinally with the impactor arm, allowing the sliding table to displace linearly for a maximum distance of 0.54 ± 0.01 m. The height of the rail system and table can also be adjusted to accommodate for impact height.

3.1.2 Striking Caps

Three striking caps of varied compliance were used to impact the headform (Fig. 4). They were composed of modular elastic programmer (MEP) and vinyl nitrile foam, that have different levels of stiffness as a result of their density. The compliance of each cap was translated into graded peak acceleration/time pulse durations between 5 ms and 30 ms. Falls to ice were represented by low compliance short event durations (5–10 ms). A mid-range event duration (10–20 ms) represented elbow collisions. Shoulder impacts were reproduced by the high compliance striking cap, resulting in the longest event durations (20-30 ms).

Fig. 4. Striking caps. From left: high, medium and low compliance striking caps.

3.1.3 University College Dublin Brain Trauma Model

To determine peak MPS for helmeted ice hockey impacts, the University College Dublin Brain Trauma Model developed by Horgan and Gilchrist (2003) was used. The model was validated against intracranial pressure data from Nahum et al. (1977) cadaver impact tests and brain motion against Hardy et al. (2001) research. The model was validated by directly comparing the predicted pressure-time histories against those obtained experimentally. The analysis was undertaken using ABAQUS. The maximum values achieved, the shape of the response and the duration of the effect all match well with that of the experimental results.

Further research was conducted comparing real-world brain injury events using the UCDBTM to anatomical data and found good agreement in ranges of MPS response (Doorly & Gilchrist, 2006). The geometry of the model was based on a male cadaver obtained by Computed Tomography (CT), Magnetic Resonance Imaging (MRI) and sliced contour photographs, available through the Visible Human Database (National Institute of Health, USA), with 0.3 mm increments in the coronal plane (Horgan & Gilchrist, 2003). The brain–skull interface was modelled using a sliding boundary condition between the skull, CSF and brain, with no space between the cerebrospinal fluid and the pia. The UCDBTM's material properties are taken from Ruan (1994), Willinger et al. (1995), Zhou et al. (1995), and Kleiven and von Holst (2002) that allows the response of the model to be within reasonable bounds of true response.

A linear viscoelastic material model combined with a large deformation theory was chosen to model the brain tissue. The behaviors of this tissue are characterized as viscoelastic in shear with a deviatoric stress rate dependent on the shear relaxation modulus (Horgan & Gilchrist, 2003). The compressive behavior of the brain is considered elastic. The hyperelastic material was used for the brain to maintain material properties consistent with Mendis et al. (1995) who constituted relationships for large deformation finite element modeling of the brain tissue, in conjunction with a viscoelastic material property as is possible in ABAQUS. The scalp, dura mater, pia mater, falx and tentorium were modeled with shell or membrane elements while the skull, CSF, cerebellum, cerebrum and brain stem were modeled with brick elements. Gray and white matter differentiation is based on MRI scans (Horgan & Gilchrist, 2004). Aspect

ratio and hourglass checks were conducted. The shear characteristic of the viscoelastic behavior is expressed through the formula:

$G(t)=G_\infty+(G_0-G_\infty)e^{-\beta t}$

Where G_∞ is the long term shear modulus, G_0 is the short term shear modulus and β is the decay factor (Horgan & Gilchrist, 2003). The hyperelastic material model used for the brain in shear was expressed as:

$C_{10}(t) = 0.9\ C_{01}(t) = 620.5 + 1930e^{-t/0.008} + 1103e^{-t/0.15}$

Where C10 and C01 are the temperatures-dependent material parameters and t is time in seconds. The results of the model are displayed as a gradient of deformation that is experienced throughout the brain tissue (Fig. 5).

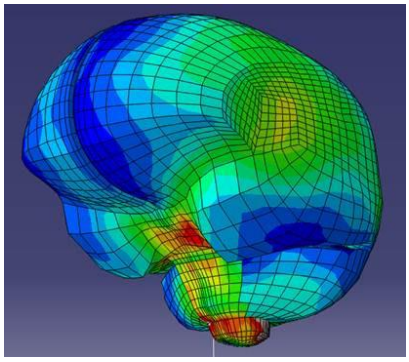

Fig 5. UCDBTM showing a gradient of high to low deformation throughout the brain.

3.1.4 Parameters used to evaluate mechanism of injuries

Different events that result in concussion create unique impact conditions that influence the direction, duration, and magnitude of the dynamic response and subsequent brain tissue stress and strains. These conditions include location and impact vector, striking velocity, and impact compliance. An increase in striking mass has a significant effect on the dynamic response of the head, in both linear and rotational acceleration (Karton, 2012). The effect of striking mass

is outside the scope of this study and it remained fixed at 13.1 kg. Impact vector and location, striking velocity, and impact compliance are the three controlled variables used in this investigation in a 5x3x3 design.

3.1.5 Impact location and Vector

Standard testing currently employs centric impact locations to evaluate helmet performance. A centric impact site is defined as the impact vector passing through the center of gravity (COG) of the head causing translational acceleration. Rotational acceleration are primarily the product of non-centric impact locations, defined as the impact vector not passing through the COG of the head inducing rotation. The influence of impact angle has also been shown to cause significant differences in the dynamic response and brain tissue deformation values while maintaining a consistent point of contact. A change of just 10-15° from a centric COG impact has been found to produce significantly higher values of linear and rotational accelerations and brain tissue deformation at front and side locations (Walsh et al., 2011; Oeur et al., 2012). Concussive injuries are closely associated with rotational accelerations of the head which is why non-centric impacts should be included when assessing helmet performance.

Table 1. University of Ottawa Test Protocol (uOTP[5]) conditions used in this study.

Site	Location	Impact angle
Front	Anterior intersection of the mid-sagittal and transverse planes	15° elevation in the mid-sagittal plane towards the impactor
Frontboss	Midpoint between the anterior mid-sagittal and right coronal planes in the transverse plane	45° rotation in the transverse plane
Side	Right intersection of the coronal and transverse planes	No vertical or horizontal rotation was applied to the vector
Rearboss	Midpoint between the posterior mid-sagittal and right coronal planes in the transverse plane	–45° rotation in the transverse plane
Rear45	Posterior intersection of the mid-sagittal and transverse planes	–45° rotation in the transverse plane

A modified version of the University of Ottawa Test Protocol (uOTP) was used for this study. The uOTP[5] was established based on the assessment of twenty-two unhelmeted location and angle variations at an impact velocity of 5.5 m/s using a linear impactor. The results of the study revealed a total of eight impact conditions that resulted in 80% risk of concussion or higher (Walsh et al., 2011). The uOTP[5] limits each location to a single impact angle to eliminate order effect during the test procedure (Post et al., 2011, Oeur et al., 2011). Due to the nature of this study, all impacts are considered non-centric as impact locations on the helmet are located above the center of mass of the head. Table 1 and figure 6 demonstrates and describe the impact locations and vector of uOTP[5].

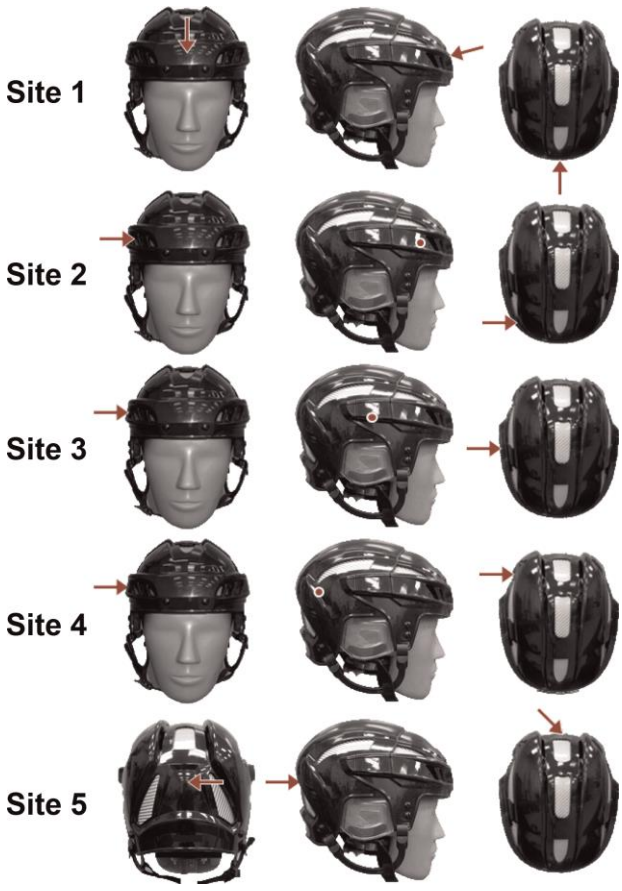

Fig 6. Impact location and angle of uOTP[5].

In hockey the impact frequency of these locations is variable. A recent study done at the Neurotrauma Impact Science Lab (NISL, University of Ottawa 2014) analyzed the mechanism of concussive injuries for elite competitive hockey players. Using video analysis, parameters such as striking velocity, location, impacting surface, and equipped helmet were determined for each case to reconstruct under a laboratory setting. The data provides insight into the real world mechanisms of concussion happening at the elite level. It was observed that Site 2 of uOTP[5] is the area on the head that has the highest impact frequency with an opponent at 40% of concussive hits occurring at this site. Other studies that used the same analysis techniques and found that 74% of impacts in hockey were in the area of Site 2 of the uOTP[5] (Rousseau, 2014).

3.1.6 Velocity

Hockey is one of the world's fastest contact sports. The low friction between the ice and skates allow players to reach high velocities. Striking velocity is a major component in the generation of force during a collision. Velocity used in the drop test for helmet certification standards ranges from 3.96-4.5 m/s which is reflective of a player's fall to the ice. Professional and senior amateur hockey players can reach on ice skating velocities ranging from an average of 11 m/s up to 18 m/s (Honey, 1998; Sim et al., 1987; Sim & Chao, 1978) Even at the pee wee level, hockey players have been recorded reaching speeds of up to 9 m/s (Sim et al., 1987). Recent investigation into hockey player collisions has revealed a lower range of velocities during concussive impacts, as well as lower collision speeds compared to other sports such as American football (9.3±1.9 m/s) (Pellman et al., 2003). This may be a reflection of the nature of each sport as the purpose of a check in hockey is to separate the opponent from the puck,

which differs from football collisions where the purpose of a tackle is to stop the opponents forward progression. Hockey players are also discouraged from having high collision velocities as they could be penalized for charging which is a reflection of the high risk of injury associated with high velocity impacts.

Video analysis of elite hockey leagues revealed an average striking velocity of 6.8 m/s for shoulder impacts, and 5.04 m/s to 5.85 m/s for elbow impacts (Rousseau, 2014). Further investigation has revealed a mean velocity of 7.8 m/s for shoulder impacts (n=34), and 6.02 m/s for elbow (n=9) in the elite level hockey (NISL, 2014). Therefore, in order to accurately represent concussive mechanisms in ice hockey, a striking velocity of 7.5 m/s was used in this study to mimic on-ice player collisions. A low end velocity of 4.5 m/s was used to match the certification testing standards. Finally a striking velocity of 6 m/s, which is equidistant between the high and low velocities, was included to monitor the progressive effect that striking velocity has on compliance, as well as to match the average striking velocity of elbow impacts.

3.1.7 Compliance

The main objective of this study was to investigate the effect of compliance on dynamic response and brain tissue strain, and how it associates with concussion risk at different levels of striking compliance. Three striking caps of varying compliance (Fig. 4) were used to impact the headform. The compliance of each cap is translated into graded peak acceleration/time durations within a range of 5 to 25 ms. These event durations represent the durations of different mechanisms of concussion in ice hockey. Falls to ice being low compliance (5-10 ms), elbow impacts/collisions as the middle compliance (10-20 ms), and shoulder impacts/collisions

having the highest compliance (20-30 ms) (Rousseau, 2014). The three caps underwent a material compliance test using an Instron measurement device in order to establish a compression rate for each cap. By gaining a better understanding impacting compliance, the mechanism of concussion can be better understood.

3.1.8 Procedure

The uOTP[5] testing procedure was run for the three levels of compliance at 4.5 m/s, 6 m/s, and 7.5 m/s (Appendix I). To ensure consistency of the impact location, a pointer attached to the end of the striking arm is used for each condition when the headform position has been modified. Three trials were performed for each condition to develop a mean and standard deviations in peak dynamic response and brain tissue strain measures. The resulting dynamic response from the reconstructions served as input into UCDBTM. This model was used to approximate the magnitude and location of brain tissue deformations experienced during the three levels of compliance. Results were then analyzed and evaluated using established percent injury risk values from the literature.

3.1.9 Statistics

Data was expressed as mean and standard deviations. The dependent variables, peak resultant linear and peak resultant rotational acceleration and MPS, were analyzed using a multivariate analysis of variance (MANOVA) to determine if there were significant differences between the three controlled variables. Partial eta squares (η_p^2) were reported to provide an estimate of the proportion of the variance that can be attributed to the tested factor. Separate ANOVAs were performed for each controlled variable to measure their effect. Bonferroni post-hoc tests were administered to determine the locus of the differences. Differences with a

probability of less than 0.05 were considered significant. All analyses were performed using the statistical software package SPSS 21 for Windows (IBM Inc., Armonk, NY, USA).

Chapter 4

4.1 Results

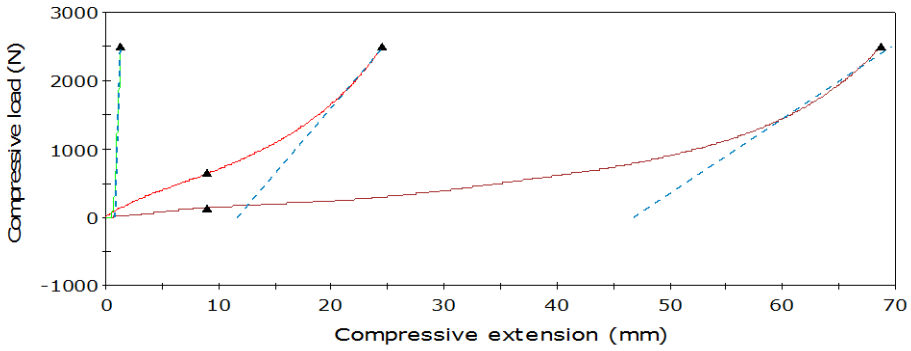

Fig 7. Instron results for the three striking caps. Low, medium, and high compliance ordered from left to right.

A materials test using an Instron was carried out on the three striking caps to determine the compression rate of each cap (Fig. 7, Table 2). Although the mid compliance striking cap is not equidistant between the low and high compliance conditions, the target impact duration was achieved using this cap.

Table 2. Instron results for the three striking caps. The modulus describes compliance when opposing forces are applied along that axis; it is defined as the ratio of tensile stress to tensile strain.

Striking Caps	Max. Stress (N/mm^2)	Max. Load (kN)	Maximum Strain (mm/mm)	Modulus (Automatic) (N/mm^2)	Compressive load at Maximum Compressive strain (N)	Time at Maximum Compressive strain (sec)
Low	0.198	2.50	0.015	**28.7**	2,503	1.594
Medium	0.197	2.50	0.283	**1.310**	2,500	29.4
High	0.197	2.50	0.793	**0.747**	2,500	82.4

Table 3. Multivariate Analysis of Variance test results.

Effect		Value	F	Hypothesis df	Error df	Sig.	Partial Eta Squared
Compliance	**Wilks' Lambda**	.002	581	6.00	176.0	**.000**	.952
Velocity	**Wilks' Lambda**	.015	211	6.00	176.0	**.000**	.878
Location	**Wilks' Lambda**	.010	91.5	12.0	233	**.000**	.785

The results of the MANOVA reveal a significant effect for compliance, velocity, and impact location for the dependent variables. There was a significant difference between the three levels of compliance for the three dependent variables, peak linear and rotational acceleration and peak MPS, Wilk's $\Lambda = .002$, $F(6, 176) = 581.89$, $p = .001$, partial $\eta^2 = .952$. There was a significant difference between the three levels of velocity for the three dependent variables, peak linear and rotational acceleration and peak MPS, Wilk's $\Lambda = .015$, $F(6, 176) = 211.26$, $p = .001$, partial $\eta^2 = .878$. There was also a significant difference between the five levels of location on the three dependent variables, peak linear and rotational acceleration and peak MPS, Wilk's $\Lambda = .010$, $F(6, 176) = 91.547$, $p = .001$, partial $\eta^2 = .785$

Table 4. Descriptive statistics of compliance at low velocity (4.5 m/s) impacts across the five impact locations.

		N	Mean	Std. Deviation	Std. Error	Min	Max
Linear Acc.	**High Compliance**	15	21.3	2.78	0.72	17.8	26.2
	Medium Compliance	15	33.3	5.78	1.49	23.6	42.1
	Low Compliance	15	79.3	15.2	3.92	59.5	103.8
Rotational Acc.	**High Compliance**	15	1972	339	87.6	1584	262
	Medium Compliance	15	306	619	159.7	1998	385
	Low Compliance	15	695	1078	278	457	811
MPS	**High Compliance**	15	0.220	0.032	0.008	0.171	0.263
	Medium Compliance	15	0.284	0.045	0.011	0.215	0.338
	Low Compliance	15	0.428	0.045	0.012	0.325	0.475

Table 5. Bonferroni Post Hoc test of compliance at low velocity (4.5 m/s) impacts across the five impact locations. The mean difference is significant at the 0.05 level.

Dependent Variable	(I) Compliance	(J) Compliance	Mean Difference (I-J)	Std. Error	Sig.	95% Confidence Interval	
						Lower Bound	Upper Bound
Linear Acc.	**High Compliance**	**Medium Compliance**	-12.02	3.48	**0.004**	-20.7	-3.35
		Low Compliance	-57.9	3.48	**0.000**	-66.6	-49.3
	Medium Compliance	**High Compliance**	12.02	3.48	**0.004**	3.35	20.7
		Low Compliance	-45.9	3.48	**0.000**	-54.6	-37.3
	Low Compliance	**High Compliance**	57.9	3.48	**0.000**	49.3	66.6
		Medium Compliance	45.9	3.48	**0.000**	37.3	54.6
Rotational Acc.	**High Compliance**	**Medium Compliance**	-1082	272	**0.001**	-1759	-405
		Low Compliance	-4980	272	**0.000**	-5660	-4300
	Medium Compliance	**High Compliance**	1082	272	**0.001**	405	1760
		Low Compliance	-3900	272	**0.000**	-4580	-322
	Low Compliance	**High Compliance**	4980	272	**0.000**	4300	5660
		Medium Compliance	3900	272	**0.000**	3220	4580
MPS	**High Compliance**	**Medium Compliance**	-0.063	0.015	**0.000**	-0.1009	-0.0260
		Low Compliance	-0.208	0.015	**0.000**	-0.246	-0.1708
	Medium Compliance	**High Compliance**	0.063	0.015	**0.000**	0.026	0.1009
		Low Compliance	-0.1447	0.015	**0.000**	-0.1822	-0.1073
	Low Compliance	**High Compliance**	0.208	0.015	**0.000**	0.1708	0.246
		Medium Compliance	0.1447	0.015	**0.000**	0.1073	0.1822

At 4.5 m/s, peak linear acceleration was significantly higher (p=0.001) for the low striking compliance compared to the medium striking compliance, with a difference of 45.96 g. Low striking compliance was also significantly higher (p=0.001) compared to the high striking compliance, with a difference in peak linear acceleration of 58.0 g. The medium striking compliance was significantly higher than the high striking compliance (p=0.004), with a

difference in peak linear acceleration of 12.0 g. Peak rotational acceleration was significantly higher (p=0.001) for the low striking compliance compared to the medium striking compliance, with a difference of 3897.8 rad/s^2. Low striking compliance was also significantly higher (p=0.001) compared to the high striking compliance, with a difference in peak rotational acceleration of 4980.2 rad/s^2. The medium striking compliance was significantly higher than the high striking compliance (p=0.006), with a difference in peak rotational acceleration of 1082.4 rad/s^2. For MPS values, the low striking compliance was significantly higher (p=0.001) compared to the medium striking compliance, with a difference of 14.5 % strain. Low striking compliance was also significantly higher (p=0.001) compared to the high striking compliance, with a difference of 20.8 % strain. The medium striking compliance was significantly higher than the high striking compliance (p=0.001), with a difference of 6.4 % strain.

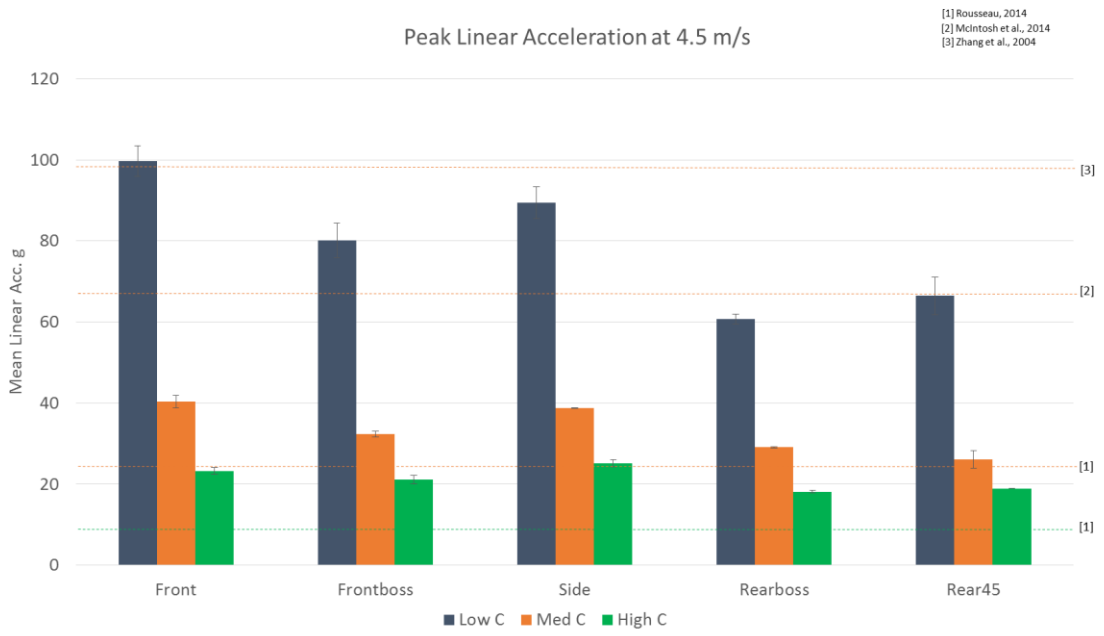

Fig 8. Peak linear acceleration for the three levels of compliance across the five impact locations at a striking velocity of 4.5 m/s. 50% injury risk is shown by the dashed lines and their respective studies. Risk duration is matched to the condition where orange is 10-20 ms (medium compliance) and green is 20 + ms (high compliance).

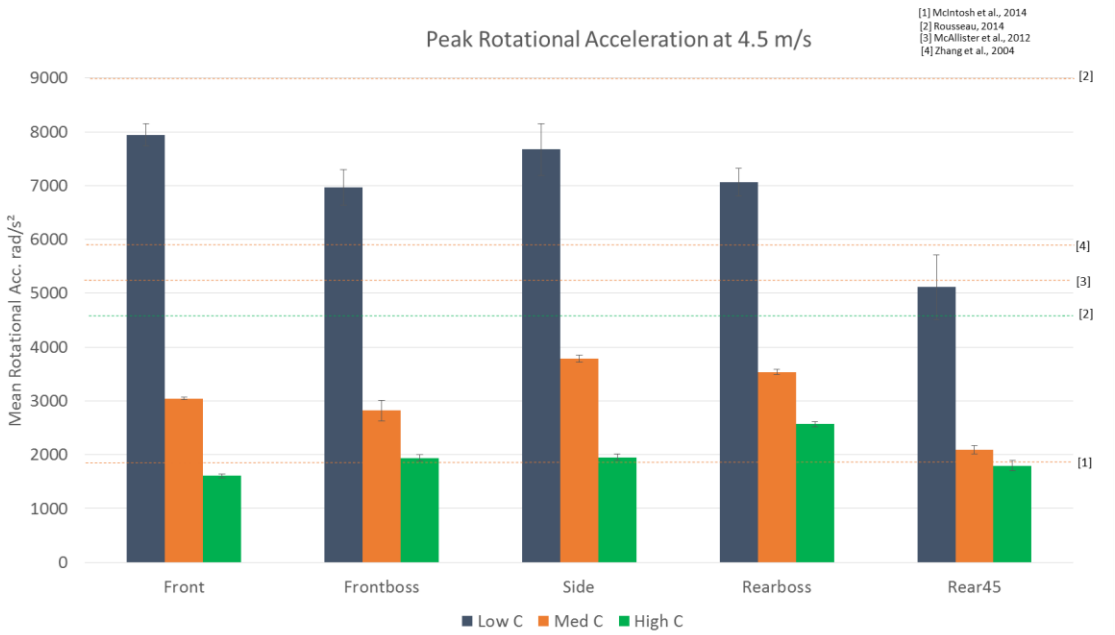

Fig 9. Peak rotational acceleration for the three levels of compliance across the five impact locations at a striking velocity of 4.5 m/s. 50% injury risk is shown by the dashed lines and their respective studies. Risk duration is matched to the condition where orange is 10-20 ms (medium compliance) and green is 20 + ms (high compliance).

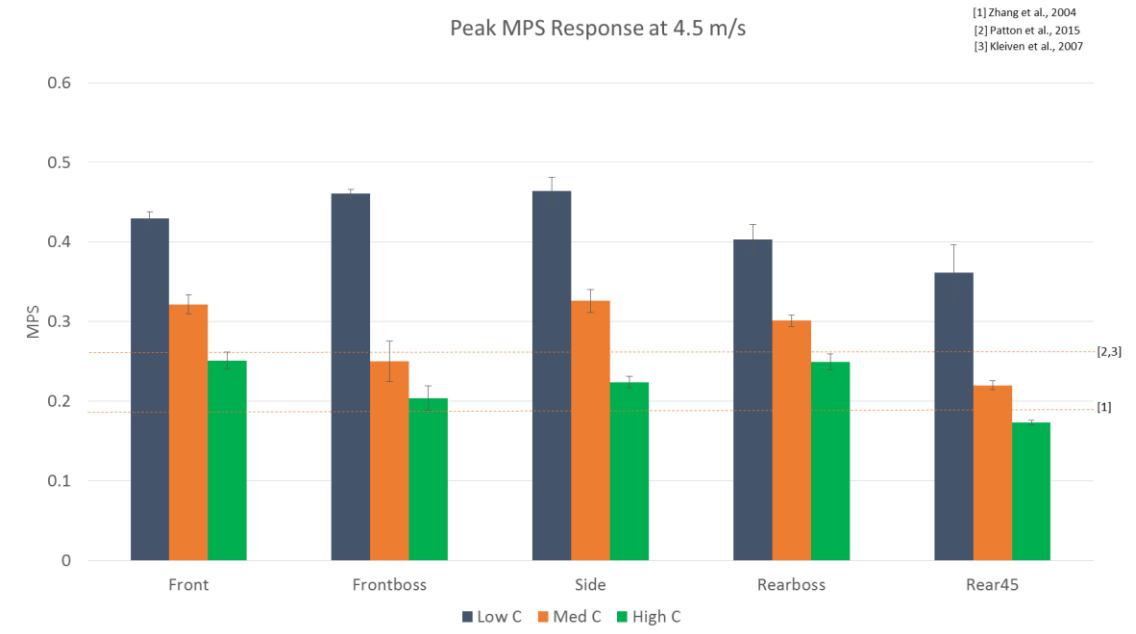

Fig 10. Peak MPS response for the three levels of compliance across the five impact locations at a striking velocity of 4.5 m/s. 50% injury risk is shown by the dashed lines and their respective studies. Risk duration is matched to the condition where orange is 10-20 ms (medium compliance) and green is 20 + ms (high compliance).

Table 6. Descriptive statistics of compliance at medium velocity (6 m/s) impacts across the five impact locations.

		N	Mean	Std. Deviation	Std. Error	Min	Max
Linear Acc.	**High Compliance**	15	25.3	4.69	1.21	18.9	32.8
	Medium Compliance	15	48.5	5.94	1.53	41.3	57.2
	Low Compliance	15	194.9	40.0	10.34	146.1	260
Rotational Acc.	**High Compliance**	15	2390	543	140.1	1747	3500
	Medium Compliance	15	4280	702	181.4	324	5269
	Low Compliance	15	17810	268	692	12870	22200
MPS	**High Compliance**	15	0.240	0.048	0.012	0.1486	0.297
	Medium Compliance	15	0.368	0.057	0.014	0.255	0.427
	Low Compliance	15	0.677	0.091	0.024	0.551	0.802

Table 7. Bonferroni Post Hoc test of compliance at medium velocity (6m/s) impacts across the five impact locations. The mean difference is significant at the 0.05 level.

Dependent Variable	(I) Compliance	(J) Compliance	Mean Difference (I-J)	Std. Error	Sig.	95% Confidence Interval	
						Lower Bound	Upper Bound
Linear Acc.	**High Compliance**	**Medium Compliance**	-23.2	8.59	**.030**	-44.6	-1.780
		Low Compliance	-169.6	8.59	**.000**	-191.0	-148.2
	Medium Compliance	**High Compliance**	23.2	8.59	**.030**	1.780	44.6
		Low Compliance	-146.4	8.59	**.000**	-167.8	-125.0
	Low Compliance	**High Compliance**	169.6	8.59	**.000**	148.2	191.0
		Medium Compliance	146.4	8.59	**.000**	124.9	167.8
Rotational Acc.	**High Compliance**	**Medium Compliance**	-1886	596	**.010**	-3370	-401
		Low Compliance	-15420	596	**.000**	-16900	-13940
	Medium Compliance	**High Compliance**	1886	596	**.001**	401	3370
		Low Compliance	-13530	596	**.000**	-15020	-12050
	Low Compliance	**High Compliance**	15420	596	**.000**	13940	16900
		Medium Compliance	13530	596	**.000**	12050	15020
MPS	**High Compliance**	**Medium Compliance**	-0.1285	0.025	**.000**	-0.1903	-0.066
		Low Compliance	-0.437	0.025	**.000**	-0.499	-0.376
	Medium Compliance	**High Compliance**	0.128	0.025	**.000**	0.066	0.1903
		Low Compliance	-0.309	0.025	**.000**	-0.371	-0.247
	Low Compliance	**High Compliance**	0.437	0.025	**.000**	0.376	0.499
		Medium Compliance	0.309	0.025	**.000**	0.247	0.371

At 6 m/s, peak linear acceleration was significantly higher (p=0.001) for the low striking compliance compared to the medium striking compliance, with a difference of 146.1 g. Low striking compliance was also significantly higher (p=0.001) compared to the high striking compliance, with a difference in peak linear acceleration of 169.6 g. The medium striking compliance was significantly higher than the high striking compliance (p=0.030), with a difference in peak linear acceleration of 23.2 g. Peak rotational acceleration was significantly

higher (p=0.001) for the low striking compliance compared to the medium striking compliance, with a difference of 13534.6 rad/s^2. Low striking compliance was also significantly higher (p=0.001) compared to the high striking compliance, with a difference in peak rotational acceleration of 15421.0 rad/s^2. The medium striking compliance was significantly higher than the high striking compliance (p=0.006), with a difference in peak rotational acceleration of 1886.4 rad/s^2. For MPS values, the low striking compliance was significantly higher (p=0.001) compared to the medium striking compliance, with a difference of 30.9 % strain. Low striking compliance was also significantly higher (p=0.001) compared to the high striking compliance, with a difference of 43.7 % strain. The medium striking compliance was significantly higher than the high striking compliance (p=0.001), with a difference of 12.8 % strain.

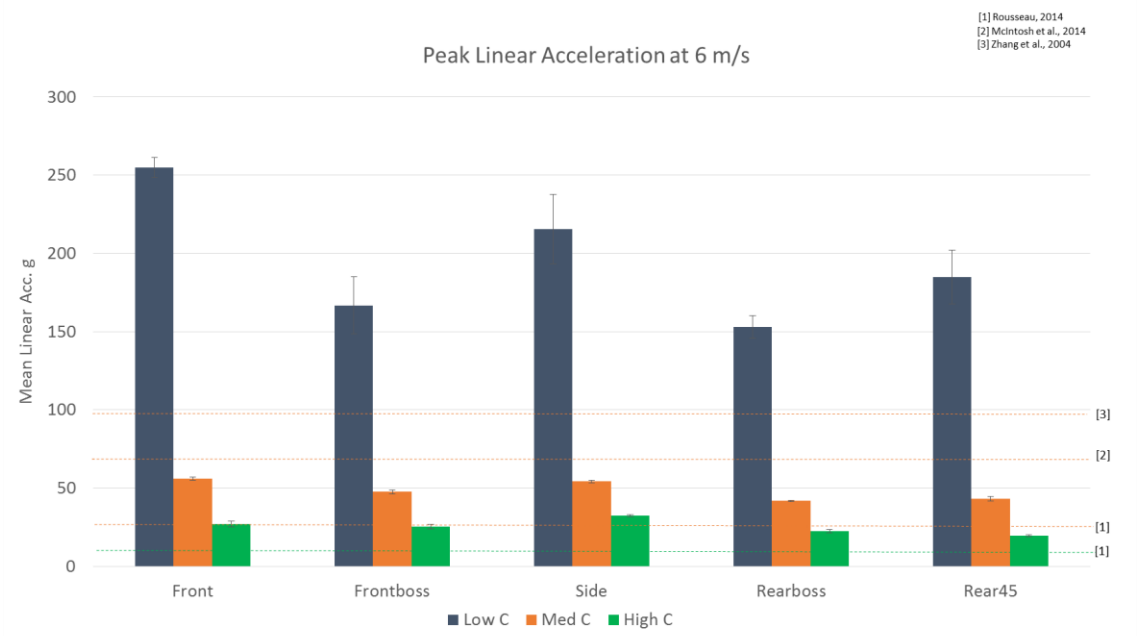

Fig 11. Peak linear acceleration for the three levels of compliance across the five impact locations at a striking velocity of 6 m/s. 50% injury risk is shown by the dashed lines and their respective studies. Risk duration is matched to the condition where orange is 10-20 ms (medium compliance) and green is 20 + ms (high compliance).

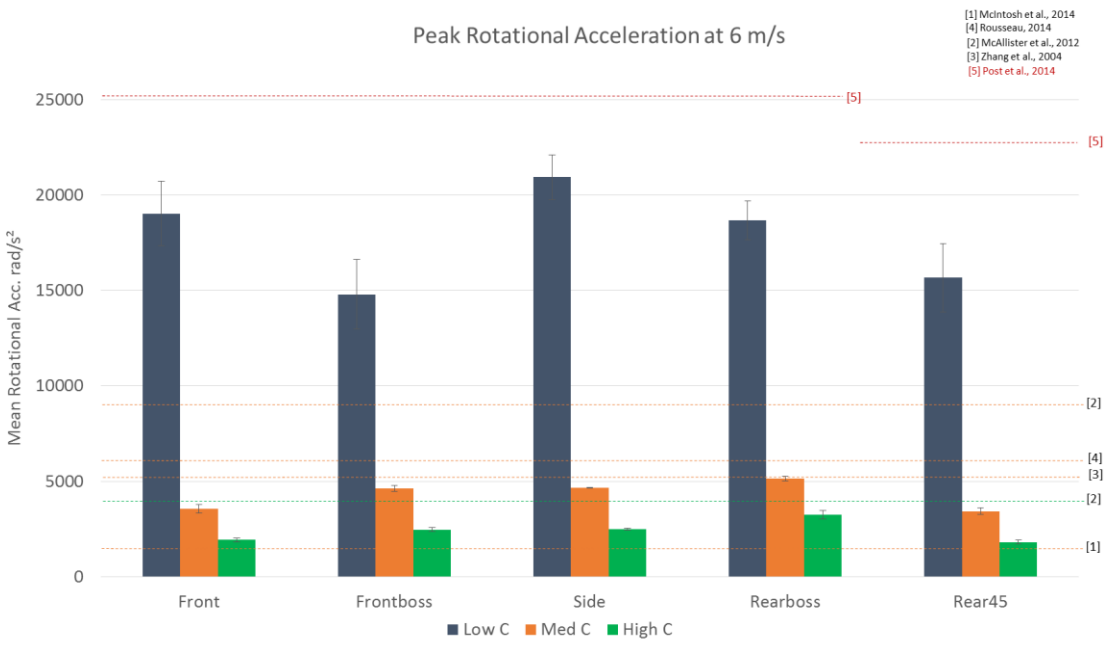

Fig 12. Peak rotational acceleration for the three levels of compliance across the five impact locations at a striking velocity of 6 m/s. 50% injury risk is shown by the dashed lines and their respective studies. Risk duration is matched to the condition where orange is 10-20 ms (medium compliance) and green is 20 + ms (high compliance). Red lines represent traumatic brain injury risk.

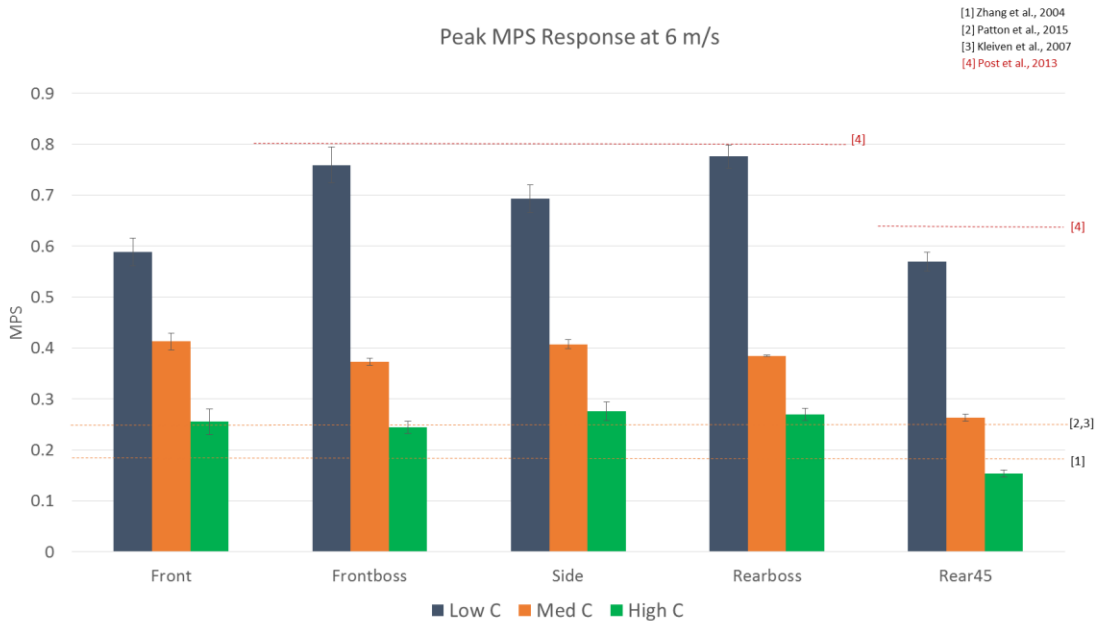

Fig 13. Peak MPS response for the three levels of compliance across the five impact locations at a striking velocity of 6 m/s. 50% injury risk is shown by the dashed lines and their respective studies. Risk duration is matched to the condition where orange is 10-20 ms (medium compliance) and green is 20 + ms (high compliance). Red lines represent traumatic brain injury risk.

Table 8. Descriptive statistics of compliance at high velocity (7.5 m/s) impacts across the five impact locations.

		N	Mean	Std. Deviation	Std. Error	Min	Max
Linear Acc.	**High Compliance**	15	37.1	5.70	1.47	28.1	46.1
	Medium Compliance	15	75.8	7.51	1.94	64.5	88.1
	Low Compliance	15	310	65.5	16.91	208	399
Rotational Acc.	**High Compliance**	15	3520	908	234	2390	5270
	Medium Compliance	15	7170	1041	269	5610	9100
	Low Compliance	15	28800	5050	1304	20200	37800
MPS	**High Compliance**	15	.336	.057	.015	.223	.403
	Medium Compliance	15	.499	.059	.015	.390	.5840
	Low Compliance	15	.982	.1830	.048	.658	1.238

Table 9. Bonferroni Post Hoc test of compliance at high velocity (7.5 m/s) impacts across the five impact locations. The mean difference is significant at the 0.05 level.

Dependent Variable	(I) Compliance	(J) Compliance	Mean Difference (I-J)	Std. Error	Sig.	95% Confidence Interval	
						Lower Bound	Upper Bound
Linear Acc.	**High Compliance**	**Medium Compliance**	-38.6	13.94	**.025**	-73.4	-3.87
		Low Compliance	-273	13.94	**.000**	-308	-238
	Medium Compliance	**High Compliance**	38.6	13.94	**.025**	3.87	73.4
		Low Compliance	-234	13.94	**.000**	-269	-199.9
	Low Compliance	**High Compliance**	273	13.94	**.000**	239	308
		Medium Compliance	234	13.94	**.000**	199.9	269
Rotational Acc.	**High Compliance**	**Medium Compliance**	-3650	1104	**.006**	-6400	-95.3
		Low Compliance	-25300	1104	**.000**	-28000	-22500
	Medium Compliance	**High Compliance**	3650	1104	**.006**	895	6400
		Low Compliance	-21600	1104	**.000**	-24400	-18890
	Low Compliance	**High Compliance**	25300	1104	**.000**	22500	28000
		Medium Compliance	21600	1104	**.000**	18890	24400
MPS	**High Compliance**	**Medium Compliance**	-.1644	.042	**.001**	-.270	-.0584
		Low Compliance	-.647	.042	**.000**	-.753	-.541
	Medium Compliance	**High Compliance**	.1644	.042	**.001**	.058	.270
		Low Compliance	-.482	.042	**.000**	-.588	-.376
	Low Compliance	**High Compliance**	.647	.042	**.000**	.541	.753
		Medium Compliance	.482	.042	**.000**	.376	.588

At 7.5 m/s, peak linear acceleration was significantly higher (p=0.001) for the low striking compliance compared to the medium striking compliance, with a difference of 234.7 g. Low striking compliance was also significantly higher (p=0.001) compared to the high striking compliance, with a difference in peak linear acceleration of 273.4 g. The medium striking compliance was significantly higher than the high striking compliance (p=0.025), with a

difference in peak linear acceleration of 38.7 g. Peak rotational acceleration was significantly higher (p=0.001) for the low striking compliance compared to the medium striking compliance, with a difference of 21644.2 rad/s^2. Low striking compliance was also significantly higher (p=0.001) compared to the high striking compliance, with a difference in peak rotational acceleration of 25293.4 rad/s^2. The medium striking compliance was significantly higher than the high striking compliance (p=0.006), with a difference in peak rotational acceleration of 3649.1 rad/s^2. For MPS values, the low striking compliance was significantly higher (p=0.001) compared to the medium striking compliance, with a difference of 48.2 % strain. Low striking compliance was also significantly higher (p=0.001) compared to the high striking compliance, with a difference of 64.7 % strain. The medium striking compliance was significantly higher than the high striking compliance (p=0.001), with a difference of 16.4 % strain.

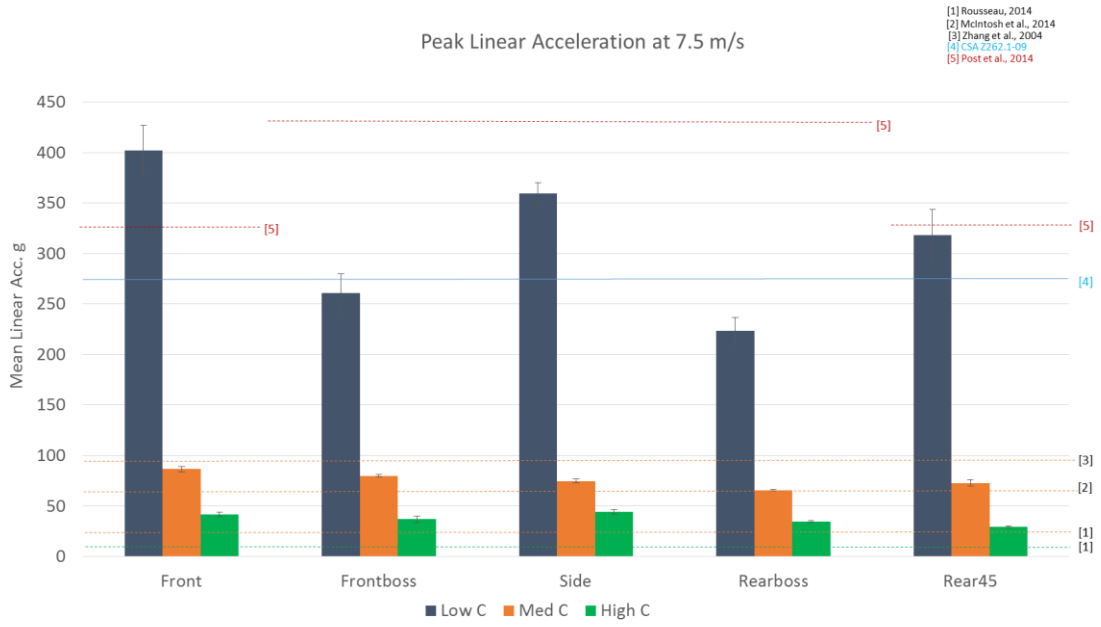

Fig 14. Peak linear acceleration for the three levels of compliance across the five impact locations at a striking velocity of 7.5 m/s. 50% injury risk is shown by the dashed lines and their respective studies. Risk duration is matched to the condition where orange is 10-20 ms (medium compliance) and green is 20 + ms (high compliance). Red lines represent traumatic brain injury risk.

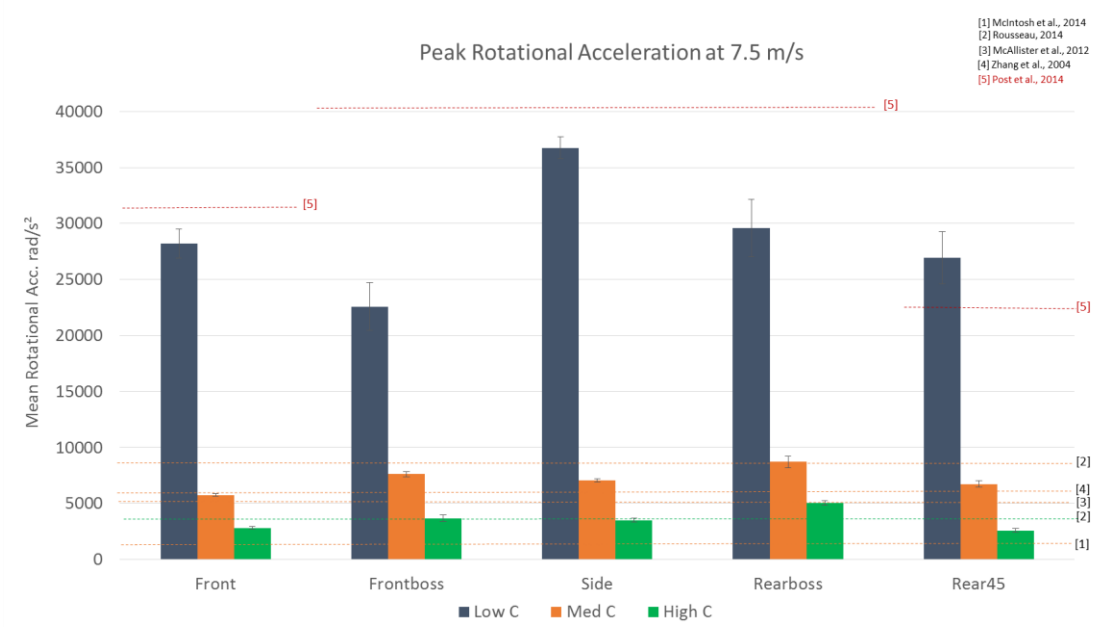

Fig 15. Peak rotational acceleration for the three levels of compliance across the five impact locations at a striking velocity of 7.5 m/s. 50% injury risk is shown by the dashed lines and their respective studies. Risk duration is matched to the condition where orange is 10-20 ms (medium compliance) and green is 20 + ms (high compliance). Red lines represent traumatic brain injury risk.

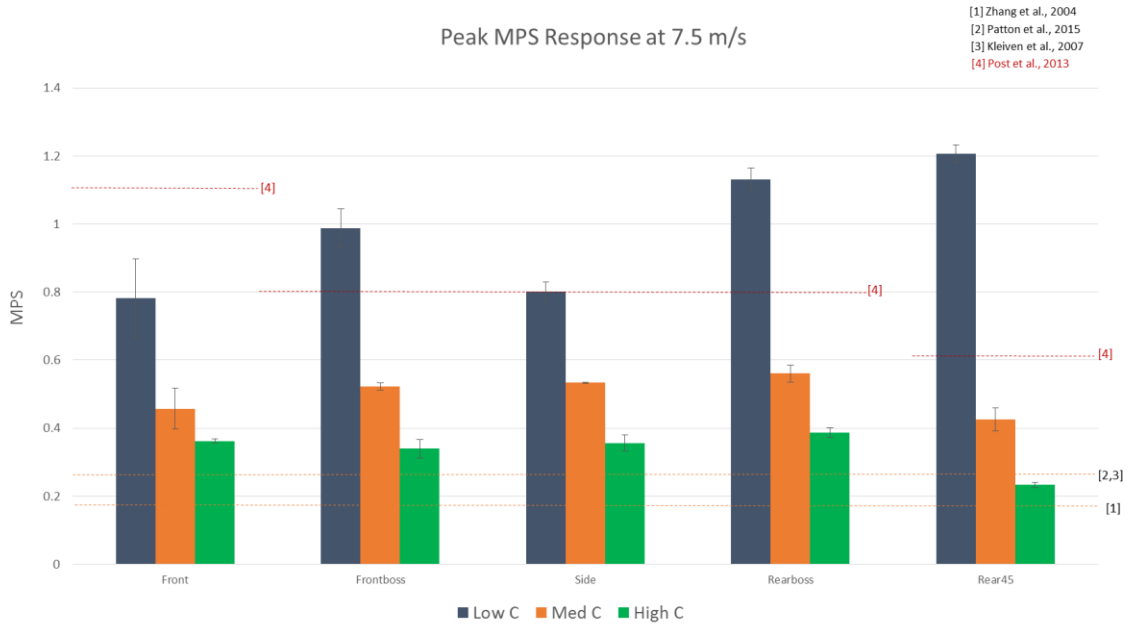

Fig 16. Peak MPS response for the three levels of compliance across the five impact locations at a striking velocity of 7.5 m/s. 50% injury risk is shown by the dashed lines and their respective studies. Risk duration is matched to the condition where orange is 10-20 ms (medium compliance) and green is 20 + ms (high compliance). Red lines represent traumatic brain injury risk.

Table 10. Percent difference of peak response values between Compliance levels.

Velocity	**Compliance**				
	High	**% Difference**	Medium	**% Difference**	Low
Linear Acc. (g)					
4.5m/s	21.3	**56.3**	33.3	**138.1**	79.3
6 m/s	25.3	**91.7**	48.5	**301.8**	194.9
7.5 m/s	37.2	**103.8**	75.8	**309.6**	310.5
Rotational Acc. (rad/s^2)					
4.5m/s	1972.6	**54.9**	3055.1	**127.6**	6952.8
6 m/s	2393.6	**78.8**	4280	**316.2**	17814.6
7.5 m/s	3523.4	**103.6**	7172.5	**301.8**	28816.7
MPS					
4.5m/s	0.2202	**28.8**	0.2837	**51.0**	0.4284
6 m/s	0.2399	**53.6**	0.3684	**83.8**	0.6772
7.5 m/s	0.3355	**49.0**	0.4998	**96.5**	0.9822

Table 11. Percent difference of peak response values between velocities.

Compliance	**Velocity**				
	4.5 m/s	**% Difference**	6 m/s	**% Difference**	7.5 m/s
Linear Acc. (g)					
High	21.3	**18.8**	25.3	**47.0**	37.2
Medium	33.3	**45.6**	48.5	**56.3**	75.8
Low	79.3	**145.8**	194.9	**59.3**	310
Rotational Acc. (rad/s^2)					
High	1973	**21.3**	2390	**47.2**	3520
Medium	3050	**40.1**	4280	**67.6**	7170
Low	6950	**156.2**	17810	**61.8**	28800
MPS					
High	.220	**8.9**	.234	**39.8**	.3350
Medium	.284	**29.9**	.368	**35.7**	.500
Low	.428	**58.1**	.677	**45.0**	.982

The results in Table 10 show the percent differences between the three compliance levels at each velocity. For peak dynamic response the difference was much larger (more than double) between the medium and low compliance levels compared to the difference between high and medium compliance levels for the three escalating velocities. MPS results demonstrated the same pattern in that the difference between medium and low compliance was larger than the difference between high and medium compliance, although these

differences were not as great from one another compared to dynamic response. Similarly, Table 11 demonstrates the percent differences as a function of velocity for each compliance level to observe the effect that velocity had on striking compliance. There is an observable difference between what occurs to low and high compliance impacts during the transition between low to mid velocity and mid to high velocity. The two conditions show opposing effects. For high compliance impacts, the difference in response values increases as the velocity increases, whereas during low compliance impacts the values decrease as velocity increases.

Table 12. Mean impact durations for high velocity and low velocity conditions across the five impact locations.

Velocity	Compliance level	Impact Duration (ms)					
		Front	Frontboss	Side	Rearboss	Rear 45	Mean
High V	**High C**	20	22	22	20	21	**21**
	Med C	13	15	14	14	14	**14**
	Low C	5	6	5	6	6	**5.6**
Low V	**High C**	24	27	27	25	26	**25.8**
	Med C	18	20	20	22	23	**20.6**
	Low C	8	12	8	10	12	**10**

Table 13. Impact duration range for each compliance level. Range of response from low to high velocity at each level of compliance.

Compliance Level	Impact Duration Range (ms)
Low Compliance	5.6-10
Medium Compliance	14-20.6
High Compliance	21-25.8

Low impact compliance conditions produced event durations ranging from 5.6 ms at high velocities to 10 ms at low velocities. This range was classified as short duration events in hockey for this study. Medium impact compliance conditions produced event durations ranging from 14 ms at high velocities to 20.6 ms at low velocities. This range was classified as mid-duration events in hockey for this study. High impact compliance conditions produced event durations ranging from 21 ms at high velocities to 25.8 ms at low velocities. This range was

classified as long duration events in hockey for this study. Examples of short and long duration events can be seen in Fig. 17. Note: Magnitude of the event is much larger for short event durations compared to longer duration events of the same mechanism (y-axis).

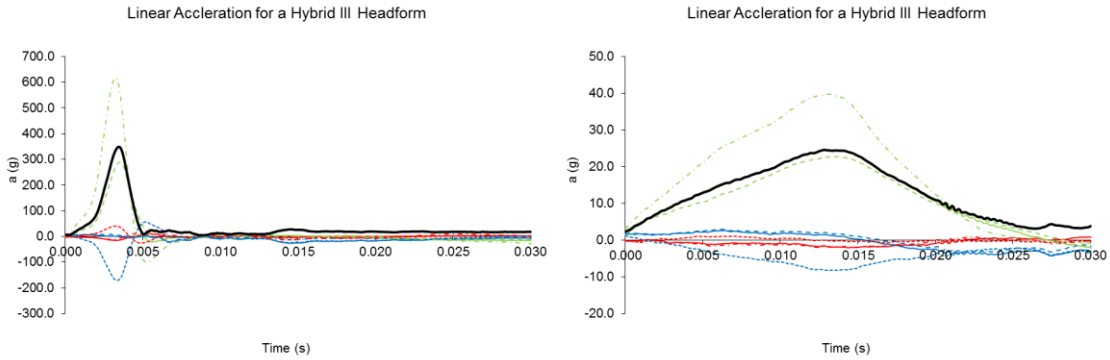

Fig 17. Acceleration time graphs that demonstrate examples of a short duration impact (left: high velocity, side, low compliance) and a long duration impact (right: low velocity, side, high compliance).

Chapter 5

5.1 Discussion

The effect of striking compliance in ice hockey impacts, and its influence on dynamic response and brain tissue strain was investigated in this study. The effect of striking compliance was significant for the three dependent variables (Table 3), and had the greatest magnitude of influence ($\eta 2 = .952$) over velocity ($\eta 2 = .878$) and location ($\eta 2 = .785$). An inverse relationship was observed between striking compliance and the dependent variable. As compliance was decreased, resultant values for all three measured variables increased. These changes however were not proportional across the three levels of compliance and the risk of brain injury associated with them. Furthermore, when the testing parameters for this study were compared to those used in standard testing (low velocity & low compliance) the helmet was effective in meeting standard certification requirements. This testing condition resulted in a mean linear acceleration of 79.3 g, well below the standard cut-off of 275 g used to certify helmets. In

hockey, players can experience a broad range of striking/surface compliance during a head impact, from the stiff ice surface to highly compliant player collisions that are not reflected in the standard. The purpose of this research was to investigate dynamic and brain tissue response under different impacting conditions representing conditions observed in hockey associated with brain trauma.

As impact compliance increased, the change in response values varied for each the dependent variables. It can be observed (Table 10) that the difference in dynamic response values between the low and medium striking compliance levels was larger than the difference between the medium and high compliance levels. This is the result of the energy distribution of an impact shifting from being fully transferred to the helmeted head upon impact in a low compliance hit, to being redistributed by the soft material of the striking surface in a high compliance hit, consequently elongating the duration of the impact. This was consistent for linear and rotational acceleration as response values more than doubled for all cases when the low compliance striker was used. The differences across compliance was the same but not as great for MPS, (Table 13). It should be noted that the differences between compliance levels for peak linear and peak rotational accelerations are almost identical across the three velocities. Rotational values are computed from the linear measurements recorded by the accelerometers which could explain the relationship across the three compliance levels.

Changes in velocity had an opposite effect between low and high compliance impacts for peak dynamic and brain tissue response values (Table 11). The percent difference in response values during high compliance impacts increased as velocity was increased. This was also true for the mid compliance level, although not to the same degree as this relationship

begins to level off. At low impact compliance, percent difference in peak dynamic response values decreases, as the change from low to mid striking velocity was higher than the change from mid to high striking velocity. This is explained again by energy being taken up by the compliant striking material during lower impact velocities. Once the transition is made to higher striking velocities, a larger difference is observed as a result of the material becoming saturated and lowering its net compliance. For the low compliance cap, the difference is larger between the low and mid velocity. Very little energy is being taken up by the stiff material of the cap and therefore the dependent variables are more susceptible to the change in velocity. Helmets are certified in the standards at 4.5 m/s so they perform well at these velocities, as is shown in the results. The helmet was effective in providing protection at a low end impact velocity, reducing the response values enough to make the difference between low and mid striking velocities larger than the transition to a high velocity impact. Mid compliance impacts remain consistent between the three velocities, although similar to the high compliance condition, the cap manages to take up some of the energy at 4.5 m/s and 6 m/s making the difference between the aforementioned velocities lower. These patterns of response are true for peak MPS values as well, though the difference between values is not as large since impact duration is taken into consideration by MPS.

The goal of protective headgear in hockey is to reduce the risk of brain injury during an impact to the head by managing the energy using both the lining and shell of the helmet. Compliance during an impact is also increased as a result of protective padding on the striking player, and physical characteristics of the human body that redistributes energy through joints and musculature. All of these factors reduce impact magnitude, but consequently increase the

duration of the event. Extended loading durations of the brain tissue have been demonstrated to increase the risk of sustaining injury and was the focus of this study. The three striking caps established an impact duration range of approximately 5-25ms that reflects what is observed in ice hockey. Furthermore, the event duration range for the individual compliance levels across the three velocities (Table 13) did not overlap and were representative of common impact durations in hockey: low compliance simulating impacts to the ice, high compliance impacts simulating player collisions, and mid-range compliance represent impacts against stiffer less padded collision scenarios such as an elbow to the head. Injury risk for the different compliance levels and event durations was determined using corresponding injury risk values from the literature.

Peak response for the dependent variables at a striking velocity of 4.5 m/s can be observed in Fig. 8, 9, and 10, along with mean injury risk values associated with concussion from the literature. Using linear acceleration as a performance metric, all response values across the five locations surpassed associated injury risk values. It is concerning that the lowest tested velocity would present such a high risk of concussive injury. And even though the helmet would pass certification testing for all compliance levels, the risk of concussion remains present. Rotational acceleration demonstrates a lower risk of injury compared to what is observed for linear acceleration. Peak rotational acceleration has been associated with concussion. The range of injury risk values is larger for rotational acceleration compared to peak linear acceleration and therefore should considered an approximation of the level of risk.

The high velocity player collisions in hockey increases risk of injury significantly. At 6 m/s, response values for peak linear, rotational, and MPS demonstrate a risk for concussion.

Once again there was a disparity between low compliance impacts and mid to high compliance conditions that decreased when analyzing the results with a FE brain model. It was also observed that at 6 m/s, peak response values for rotational acceleration and MPS near TBI risk. At 7.5 m/s, a common skating and collision velocity in elite hockey, TBI risk is surpassed for low compliance conditions in specific loading directions. Front (Site 1) and Rear45 (Site 45) low compliance impacts resulted in peak linear acceleration values that surpass TBI risk. For peak rotational acceleration, the Rear45 (Site 4) impact loading at low compliance reflected a risk for TBI. Using MPS as a risk metric demonstrated an increase in risk of injury, and four out of the five locations (excluding front) demonstrated TBI risk at the low compliance condition. This injury is rarely observed in hockey as compliance dramatically decreases the risk of TBI. The results of this study demonstrate that the majority of hockey impacting mechanisms from low to high compliance, reflect a risk in concussion, demonstrating a limitation in helmet protection for concussion.

Impact locations included in this study were not centric as all were located above the COG of the head. The impact vectors for front and side have the shortest displacement to the COG that results in more of the impact energy being transferred to the head, consequently eliciting higher peak linear acceleration compared to the other locations. This relationship stayed constant across the three velocities. Non-centric impacts at sites 2, 4 and 5 where the vector displacement is further away from the COG, produced conditions resulting in larger rotations of the head around the transverse axis. The impacts glanced off the helmet and followed through after making contact with the head. It was predicted that these impact sites would produce higher peak rotational accelerations. At 4.5 m/s Front and Side impact sights

still produced higher responses in peak rotational acceleration, though front boss and rear boss were within 1000 rad/s^2 for the low striking compliance. Site 4 was lower than all other locations. At 6m/s, sites 1 and 3 again produced the largest mean response along with site 4. Site 2 demonstrated to have the lowest response even though during testing it resulted in the largest rotational displacement of the head around the transverse axis. Finally, at 7.5 m/s site 2 produced peak rotational acceleration values of over 5000 rad/s^2 above sites 1 and 4 for the low striking compliance, with site 2 again producing the lowest peak rotational acceleration. Therefore peak rotational acceleration patterns changed as velocity was increased. The results also demonstrate that rotations around frontal and sagittal axes had a higher influence on increasing response values compared to the transverse axis as predicted. This also supports the importance of using a directionally unbiased neck to measure rotational acceleration values as a Hybrid III neck form may dampen the dynamic rotations around the sagittal and transverse axes. It was observed that the differences in peak dynamic response between locations were greater in low impact compliance conditions. For high compliance the mean response values between locations were almost negligible in terms of differences in injury risk.

Differences in MPS across the five impact locations were lower compared to differences in dynamic response conditions for the three compliance levels. As velocity was increased to 6 m/s, MPS response values for lateral impacts (Site: 2, 3, 4, Fig. 6) produced slightly higher responses at the low compliance level. Peak response remained the same for the medium and high compliance. Site 4 produced the lowest response for the five locations across the three levels of compliance. At a high impacting velocity, mid and high compliance response values still remain constant across the five locations, with Rear45 producing only a slightly lower response.

The opposite is true for the low compliance condition. This is probably not a function of the directional loading but of a point where the high dynamic responses leads to a saturation effect in the model. Low compliance impacts at such a high velocity produce a large amount of energy and consequent brain tissue response (MPS>1.0), outside of the range with which the model was developed. Therefore, the use of a brain model when such high impacting energy conditions are reached might provide limited information.

Response at each location differs as a result of head and helmet geometry. The topography of the helmet will influence how the striking surface interacts with the head, especially during high compliance impacts. Rigid structures on the helmet may increase the friction of the impact during a high compliance event, increasing the transfer of energy into the head. A single model certified hockey helmet (CSA, HECC) was used for all conditions in this study. Variance between helmet structures during high compliance impacts should be further investigated in future research as it may play an important role in the interaction between the striking surface and consequent dynamic response of the head. Furthermore, the uOTP[5] was developed using an unhelmeted headform. The determination of high risk impact sites specific to ice hockey would be beneficial when investigating concussion risk.

Compliance has not been considered in helmet design and safety certification testing for ice hockey and therefore the implications of this study can be used to improve helmet technology. Furthermore, ice hockey is one of many sports that includes impacts to the head during gameplay against variable compliant surfaces. Football, rugby, soccer, and many more include the risk of an impact to head against a low compliant surface such as a fall to ground or a high compliance impacting scenario of a collision with an opponent. Therefore, the effects of

compliance deducted from this study can be extrapolated to other contact sports and are not limited to ice hockey. Differences in protective equipment, or lack thereof, across different sports is a factor that should be further investigated.

5.1.1 Summary

The effects of striker compliance on dynamic response and brain tissue strain on a helmeted Hybrid III headform was investigated at different levels of velocity chosen to replicate on ice collisions. Compliance demonstrated to have a significant effect on dynamic and brain tissue response across the five impact locations. As compliance was increased, the magnitude of the dynamic response values decreased and the duration of the event was elongated. This elicited increased response values for MPS, within the range of concussion risk across all tested conditions. Velocity also demonstrated to have a significant effect on dependent variables, and even at the lowest tested velocity risk of concussion is present. As velocity was increased, there was an increase in the response values for the three dependent variables and consequently an increase in risk of brain injury.

In order to mitigate the risk of concussion, helmet standard test methods should consider injury mechanisms specific to concussions in ice hockey. The results of this study describe the importance of including testing parameters that replicate impacts involving high compliance surfaces, as well as including testing velocities that reflect player collisions. The results of this study provide an understanding of the limitations of ice hockey helmets in protecting against concussion from player collisions. The limitations of using peak linear acceleration as the only performance metric was also described in this research. Peak rotational acceleration and peak MPS response will provide further insight in predicting brain injury risk

across all levels of striking compliance. The result of this research also provides insight as to the limits of helmets in protecting against high velocity impacts presently experienced in ice hockey.

References

Anderson, R.W.G., Brown, C.J., Blumbergs, P.C., Scott, G., Finney, J.W., Jones, N.R., and McLean, A.J. (1999). Mechanics of axonal injury: An experimental and numerical study of a sheep model of head impact, *Proc. 1999 IRCOBI Conf.* Sitges, Spain, pp. 107-120.

Bailes, J. E. & Cantu, R. C. (2001). Head injury in athletes, *Neurosurgery*, **48**: pp. 26-46.

Bain, B.C., Billiar, K.L., Shreiber, D.I., McIntosh, T.K., & Meaney, D.F. In vivo mechanical thresholds for traumatic axonal damage. *Proc. of AGARD AMP Specialists' Meeting,* Mescalero, New Mexico, USA, November 1996, published in CP-597.

Bain, B.C., and Meaney, D.F. (2000). Tissue-Level Thresholds for Axonal Damage in an experimental Model of Central Nervous System White Matter Injury. *J. Biomech. Engng.***16**: pp. 615-622.

Baumgart, F. (2000). Stiffness - an unknown world of mechanical science? Injury-International Journal of the Care of the Injured, **31**: pp. 14-23.

Benson, B., Meeuwisse, W., Rizos, J., Kang, J., & Burke, C. (2011). A prospective study of concussions among national hockey league players during regular season games: The NHL-NHLPA concussion program. *CMAJ: Canadian Medical Association Journal, **183***(8): pp. 905-911.

Brainard, L. L., Beckwith, J. G., Chu, J. J., Crisco, J. J., Mcallister, T. W., Duhaime, A., et al. (2012). Gender differences in head impacts sustained by collegiate ice hockey players. *Medicine and Science in Sports and Exercise,* **44**(2): p. 297.

Casson, I. R., Viano, D. C., Powell, J. W., & Pellman, E. J. (2010). Twelve years of national football league concussion data. *Sports Health,* **2**(6): p. 471.

Cattelani, R., Gugliotta, N., Maravita, A., & Mazzucchi, A. (1996). Post-concussive syndrome: Paraclinical signs, subjective symptoms, cognitive functions and MMPI profiles. *Brain Injury,* **10**(3): pp. 187-195.

Collins, M., Iverson, G. et al. (2003). On-field predictors of neuropsychological and symptom deficit following sports-related concussion. Clin J Sport Med, **13**(4): pp.222–9.

Coulson, N., Foreman, S., & Hoshizaki, T. (2009). Translational and rotational accelerations generated during reconstructed ice hockey impacts on a hybrid III head. *Journal of ASTM International,* **6**(2).

Daneshvar, D. H., Riley, D. O., Nowinski, C. J., McKee, A. C., Stern, R. A., & Cantu, R. C. (2011). Long-term consequences: Effects on normal development profile after concussion. *Physical Medicine and Rehabilitation Clinics of North America,* **22**(4): 683.

Delaney, J.S., Lacroix, V.J., Leclerc, S., & Johnston, K.M. (2002). Concussions among university football and soccer players, *Clinical Journal of Sport Medicine*, **12**: pp. 331-338.

Doorly, M. C. & Gilchrist, M. D. (2006). The analysis of traumatic brain injury due to head impacts arising from falls using accident reconstruction, *Computer Methods in Biomechanics and Biomedical Engineering*, ***9***: pp. 371-377.

Doorly, M. & Gilchrist, M. (2006). The use of accident reconstruction for the analysis of traumatic brain injury due to head impacts arising from falls. Computer Methods in Biomechanics and Biomedical Engineering, **9**(6): pp.371–7.

Emery, C. A., & Meeuwisse, W. H. (2006). Injury rates, risk factors, and mechanisms of injury in minor hockey. *The American Journal of Sports Medicine,* **34**(12): p. 1960.

Forero Rueda, M. A., Cui, L., & Gilchrist, M. D. (2011). Finite element modelling of equestrian helmet impacts exposes the need to address rotational kinematics in future helmet designs. *Computer Methods in Biomechanics and Biomedical Engineering,* **14**(12): pp. 1021-1031.

Galbraith, J. A., Thibault, L. E. & Matteson, D. R. (1993). Mechanical and Electrical Responses of the Squid Giant Axon to Simple Elongation. *J. Biomech. Eng*, **115**: pp. 13–22.

Gennarelli, T. (1983) Head injury in man and experimental animals: clinical aspects. Acta Neurochir Suppl, **32**: pp.1–13.

Gennarelli, T. A., Abel, J.M., Adams, H., et al. (1979). Differential tolerance of frontal and temporal lobes to contusion induced by angular acceleration. In: 23rd Stapp Car Crash Conference, Warrendale, PA, SAE paper 791022.

Gennarelli, T. A., Thibault, L.E. & Ommaya, A. (1971). Comparison of translational and rotational accelerations in experimental cerebral concussion. In: 15th Stapp Car Crash Conference, New York, USA.

Gennarelli, T. A., Thibault, L. E. & Ommaya, A. (1972). Pathophysiological responses to rotational and translational accelerations of the head. In: 16th Stapp Car Crash Conference, Detroit, Ml, USA, SAE paper 720970.

Gennarelli, T. A., Thibault, L. E., Adams, J. H., Graham, D. I., Thompson, C. J., & Marcincin, R. P. (1982). Diffuse axonal injury and traumatic coma in the primate. *Annals of Neurology,* **12**(6): pp. 564-574.

Gennarelli, T.A., Thibault, L.E., Tipperman, R., et al. (1989). Axonal Injury in the Optic Nerve: A model of Diffuse Axonal Injury in the brain. *J. Neurosurg*. **71**: pp. 244-253.

Gerberich, S. G., Priest, J. D., Boen, J. R., Straub, C. P., & Maxwell, R. E. (1983). Concussion incidences and severity in secondary school varsity football players. *American Journal of Public Health,* **73**(12): p. 1370.

Gilchrist, M. D. (2003). Modelling and accident reconstruction of head impact injuries. Key Engineering Materials, **245**: pp.417-430.

Gilchrist, M., O'Donoghue, D., & Horgan, T. (2001). A two-dimensional analysis of the biomechanics of frontal and occipital head impact injuries. *International Journal of Crashworthiness, **6***(2), 253-262.

Goldsmith, W. & Plunkett, J. (2004). A biomechanical analysis of the causes of traumatic brain injury in infants and children, *The American Journal of Forensic Medicine and Pathology*, **25**: pp. 89-100.

Gurdjian, E. S., Roberts, V. L. & Thomas, L.M. (1966). Tolerance curves of acceleration and intracranial pressure and protective index in experimental head injury. *Journal of trauma*, ***6***(5): 600-604.

Gurdjian, E. S. & Gurdjian, E. S. (1975). Re-evaluation of the biomechanics of blunt impact injury of the head. *Surgery, Gynecology and Obstetrics,* **140**(6): 845–850.

Gurdjian, E. S. & Gurdjian, E. S. (1980). Acute head injury: a review. *Annals of Surgery,* **12**: pp. 223–241.

Gurdjian, E. S., Hodgson, V. R., Thomas, L. M., et al. (1968). Significance of relative movements of scalp, skull, and intracranial contents during impact injury to the head. *Journal of Neurosurgery,* **29**(1): pp. 70–72.

Gurdjian, E. S., & Lissner, H. R. (1945). Mechanism of head injury as studied by the cathode ray oscilloscope. *The Journal of Nervous and Mental Disease, **102***(4): pp. 425-425.

Gurdjian, E., Lissner, H., Latimer, F., Haddad, B. and Webster, J. (1953). Quantitative determination of acceleration and intracranial pressure in experimental head injury; preliminary report. Neurology, **3**(6): p.417.

Gurdjian, E., Lissner, H., Webster, J., Latimer, F. and Haddad, B. (1954). Studies on experimental concussion: Relation of physiologic effect to time duration of intracranial pressure increase at impact. Neurology, **4**(9): p.674.

Haddad, B. F., Lissner, H. R., Webster, J. E. & Gurdjian, E. S. (1955). Experimental concussion; relation to acceleration to physiologic effect. *Neurology*, **5**(11): pp. 798-800.

Hardy, W. N., Khalil, T. B., & King, A. I. (1994). Literature review of head injury biomechanics. *International Journal of Impact Engineering,* **15**(4), 561-586.

Hardy, W.N., Foster, C.D., Mason, M.J., Yang, K.H., King, A.I. & Tashman S. (2001). Investigation of head injury mechanisms using neutral density technology and high-speed biplanar X-ray. Stapp Car Crash J [The Stapp Association, Ann Arbor, Michigan].

Hodgson, V. and Thomas, L. Effect of Long-Duration Impact on Head. SAE Technical Paper, 1972, doi: 10.4271/720956.

Hardy, W.N., Foster, C.D., King, A.I., Tashman, S. (1997). Investigation of brain injury kinematics: Introduction of a new technique. Crashworthiness. Occupant Protection and Biomechanics in Transportation Systems AMD. **225**: pp. 241–254.

Hodgson, V.R., Gurdjian, E.S., Thomas, L.M. (1966). Experimental skull deformation and brain displacement demonstrated by flash x-ray technique. *Journal of Neurosurgery. **25**(5):pp.549-52.*

Holbourn, A. H. S. (1943). Mechanics of head injury. *The Lancet,* **242**: pp. 438-441.

Honey, C. R. (1998). Brain injury in ice hockey. *Clinical Journal of Sport Medicine: Official Journal of the Canadian Academy of Sport Medicine,* **8**(1): p. 43.

Horgan, T. and Gilchrist, M. (2003). The creation of three-dimensional finite element models for simulating head impact biomechanics. International Journal of Crashworthiness, **8**(4): pp.353–66.

Horgan, T., & Gilchrist, M. D. (2004). Influence of FE model variability in predicting brain motion and intracranial pressure changes in head impact simulations. *International Journal of Crashworthiness,* **9**(4): pp. 401-418.

Hoshizaki, B. & Brien, S. (2004). The science and design of head protection in sport. Neurosurgery, **55**(4): pp. 856–966.

Hubbard, R.P., McLeod, D.G. Definition and Development of a Crash Dummy Head. Proceedings of the 18th Stapp Car Crash Conference. 1974; SAE 741193.

Hutchison, M., Comper, P., Meeuwisse, W., & Echemendia, R. (2015). A systematic video analysis of National Hockey League (NHL) concussions, part I: Who, when, where and what? *British Journal of Sports Medicine*, **49**(8): pp. 547-51.

Hutchison, M., Comper, P., Meeuwisse, W., & Echemendia, R. (2015). A systematic video analysis of National Hockey League (NHL) concussions, part II: How concussions occur in the NHL. *British Journal of Sports Medicine*, **49**(8): 552-5.

Karceski, S. (2011) Patient page. Concussion. *Neurology,* **76**(17): p. 83.

Karton, C. & Hoshizaki, T.B. (2012). The effect of inbound mass on the dynamic response of the hybrid III headform and brain tissue deformation. Master's thesis dissertation, University of Ottawa, Ottawa.

King, A., Yang, K., Zhang, L., & Hardy, W. Is head injury caused by linear or angular acceleration? *IRCOBI Conference, 2003, Lisbon, Portugal.*

Kendall, M., Post, A. et al. A comparison of dynamic impact response and brain deformation metrics within the cerebrum of head impact reconstructions representing three mechanisms of head injury in ice hockey. Proceedings of the IRCOBI conference, 2012, Dublin, Ireland.

Kleiven, S. & Hardy, W. N. (2002). Correlation of an FE model of the human head with local brain motion – Consequences for injury prediction. *Stapp Car Crash Journal,* **46**: pp. 123–144.

Kleiven, S., & Von Holst, H. (2002). Consequences of head size following trauma to the human head. *Journal of Biomechanics,* **35**(2): pp. 153-160.

Kleiven, S. (2003). Influence of impact direction on the human head in prediction of subdural hematoma. *Journal of Neurotrauma,* **20**(4): p. 365.

Kleiven, S. Influence of direction and duration of impacts to the human head evaluated using the finite element method. Proceedings of IRCOBI Conference, 2005, Prague, Czech Republic, pp. 41–57.

Kleiven, S. (2006). Evaluation of head injury criteria using a finite element model validated against experiments on localized brain motion, intracerebral acceleration, and intracranial pressure. *International Journal of Crashworthiness,* **11**(1): pp. 65–79.

Kleiven, S. Predictors for traumatic brain injuries evaluated through accident reconstruction. Stapp Car Crash Journal, 2007, **51**: pp.81–114.

Koh, J., Cassidy, J., & Watkinson, E. (2003). Incidence of concussion in contact sports: A systematic review of the evidence. *Brain Injury*, **17**: pp.901–17.

LaPlaca, M. C., Lee, V., & Thibault, L.E. (1997). An in vitro model of traumatic neuronal injury: Loading rate dependent changes in acute cytosolic calcium and lactate dehydrogenase release, *Journal of Neurotrauma*, **14**: pp. 355-368

Langlois, J., Rutland-Brown, W., and Wald, M. (2006). The epidemiology and impact of traumatic brain injury: A brief overview. The Journal of Head Trauma Rehabilitation **21**(5): p.375.

Levy, M. L., Ozgur, B. M., Berry, C., Aryan, H. E., & Apuzzo, M. L. J. (2004). Analysis and evolution of head injury in football. *Neurosurgery, **55***(3): 649.

Margulies, S. S., & Thibault, L. (1992). A proposed tolerance criterion for diffuse axonal injury in man. *Journal of Biomechanics; J.Biomech.,* **25**(8): pp. 917-923.

McAllister TW, Ford JC, Ji S, et al. (2012). Maximum principal strain and strain rate associated with concussion diagnosis correlates with changes in corpus callosum white matter indices. Ann Biomed Eng; **40**:127–40.

McIntosh, A., Patton, D. et al. (2014). The biomechanics of concussion in unhelmeted football players in Australia: A case–control study. BMJ Open, **4**(5).

Mckee, C., A., Cantu, C., R., Nowinski, J., C., Hedley-Whyte, E., Gavett, E., B., Budson, E., A., et al. (2009). Chronic traumatic encephalopathy in athletes: Progressive tauopathy after repetitive head injury. *Journal of Neuropathology and Experimental Neurology,* **68**(7): pp. 709-735.

Mckee, A., Gavett, B., Stern, R., Nowinski, C. J., Cantu, R. C., Kowall, N., et al. (2010). TDP-43 proteinopathy and motor neuron disease in chronic traumatic encephalopathy. *Journal of Neuropathology and Experimental Neurology,* **69**(9): pp. 918-929.

Meaney, D. F., & Smith, D. H. (2011). Biomechanics of concussion. *Clinics in Sports Medicine,* **30**(1): 19-31.

Mori, T., Katayama, Y. and Kawamata, T. (2006). Acute hemispheric swelling associated with thin subdural hematomas: Pathophysiology of repetitive head injury in sports. Acta Neurochir Suppl, **96**: pp.40–43.

Nahum, A., Smith, R. and Ward, C. Intracranial pressure dynamics during head impact. 21st Stapp Car Crash Conference, 1977, New Orleans, USA.

Oeur, A. & Hoshizaki, T.B. (2012). An analysis of head impact angle on the dynamic response of a hybrid III headform and brain tissue deformation. Master's thesis dissertation, University of Ottawa, Ottawa.

Oeur A, Post A, Hoshizaki TB, et al. The correlation between brain deformation metrics and acceleration using a linear and non-linear impact protocol. International Society of Biomechanics conference, 2011, Brussels, Belgium.

Ommaya, A. K., & Gennarelli, T. A. (1974). Cerebral concussion and traumatic unconsciousness. correlation of experimental and clinical observations of blunt head injuries. *Brain : A Journal of Neurology,* **97**(4), 633.

Ommaya, A.K., Yarnell, P., Hirsch, A.E., et al. Scaling of experimental data on cerebral concussion in sub-human primates to concussion threshold for man. In: 11th Stapp Car Crash Conference, 1967, Anaheim, FL, USA.

Ono, K., Kikuchi, M., & Nakamura, H. Human head tolerance to sagittal impact reliable estimation deduced from experimental head injury subhuman primates and human cadaver skull. In: *24th STAPP Car Crash Conference,1980,* Troy, MI, USA.

Padgaonkar, A., Kreiger, K., King, A. (1975). Measurements of angular accelerations of a rigid body using linear accelerometers. Journal of Applied Mechanics, **42**: pp.552–6.

Patton, D., McIntosh, A. and Kleiven, S. (2015). The Biomechanical Determinants of Concussion: Finite Element Simulations to Investigate Tissue-Level Predictors of Injury during Sporting Impacts to the Unprotected Head. *Journal of Applied Biomechanics*, **31**(4): pp.264–8.

Pellman, E. J., Viano, D. C., Tucker, A. M., & Casson, I. R. (2003). Concussion in professional football: Location and direction of helmet impacts – Part 2, *Neurosurgery*, **53**: pp.1328-1341.

Post, A., Hoshizaki, T. & Gilchrist, M. (2012). Finite element analysis of the effect of loading curve shape on brain injury predictors. *Journal of Biomechanics*, **45**(4): pp.679–83.

Post, A., Hoshizaki, T. et al. (2014). The influence of dynamic response and brain deformation metrics on the occurrence of subdural hematoma in different regions of the brain: Laboratory investigation. *Journal of Neurosurgery*, **120**(2): pp.453–61.

Post, A., Blaine Hoshizaki, T., Gilchrist, M. D., Brien, S., Cusimano, M. D., & Marshall, S. (2014). The influence of acceleration loading curve characteristics on traumatic brain injury. *Journal of Biomechanics,* **47**(5): pp. 1074-1081.

Post, A., & Hoshizaki, T. B. (2012). Mechanisms of brain impact injuries and their prediction: A review. *Trauma, **14***(4): pp. 327-349.

Post, A., Hoshizaki, T. B., Gilchrist, M. D., Brien, S., Cusimano, M. D., & Marshall, S. (2014). The influence of dynamic response and brain deformation metrics on the occurrence of subdural hematoma in different regions of the brain. *Journal of Neurosurgery,* **120**(2): 453.

Post, A., Oeur, A., Hoshizaki, B., & Gilchrist, M. D. (2013). Examination of the relationship between peak linear and angular accelerations to brain deformation metrics in hockey helmet impacts. *Computer Methods in Biomechanics and Biomedical Engineering,* **16**(5): pp. 511-519.

Post, A., Oeur, A., Hoshizaki, B., & Gilchrist, M. D. (2013). Examination of the relationship between peak linear and angular accelerations to brain deformation metrics in hockey helmet impacts. *Computer Methods in Biomechanics and Biomedical Engineering,* **16**(5): pp. 511-519.

Post, A., Hoshizaki, T. et al. (2015) Traumatic Brain Injuries: The Influence of the Direction of Impact. Neurosurgery, **76**(1): pp.81–91.

Post, A., Hoshizaki, T. et al. (2015). The dynamic response characteristics of traumatic brain injury. Accident Analysis and Prevention, **79**: pp. 33–40.

Post, A., Rousseau, P., Kendall, M., Walsh, E. S., & Hoshizaki, T. B. (2015). Determination of high-risk impact sites on a hybrid III headform by finite element analysis. *Proceedings of the Institution of Mechanical Engineers, Part P: Journal of Sports Engineering and Technology,* **229**(1), pp. 17-27.

Prange, M.T., Meaney, D.F. & Margulies, S.S. Defining brain mechanical properties: Effects of region, direction and species. In: *44th Stapp Car Crash Conference*, 2002, Atlanta, GA, USA.

Quinney, H. A., Dewart, R., Game, A., Snydmiller, G., Warburton, D., & Bell, G. (2008). A 26 year physiological description of a national hockey league team. *Applied Physiology, Nutrition, and Metabolism,* **33**(4): p. 753.

Rousseau, P. & Hoshizaki, T. B. (2004). Analysis of Concussion Metrics of Real-world Concussive and Non-injurious Elbow and Shoulder to Head Collisions in Ice Hockey. PhD Thesis, University of Ottawa, Ottawa.

Rousseau, P., Post, A., & Hoshizaki, T. B. (2009). A comparison of peak linear and angular headform accelerations using ice hockey helmets. *Journal of ASTM International,* **6**(1).

Ruan, J. (1994). Impact Biomechanics of head injury by mathematical modelling. PhD thesis, Wayne State University.

Shreiber, D.I., Bain, A.C. & Meaney D.F. In vivo thresholds for mechanical injury to the blood-brain barrier. SAE Paper No. 973335, in*: 41st Stapp Car Crash Conf.*, Society of Automotive Engineers, 1997, pp. 177-190.

Sim, F., & Chao, E. (1978). Injury potential in modern ice hockey. *American Journal of Sports Medicine, **6***(6): pp. 378-384.

Sim, F., Simonet, W., Melton, L., & Lehn, T. (1987). Ice hockey injuries. *American Journal of Sports Medicine,* **15**(1): pp. 30-40.

Strich, S. (1961). Shearing of nerve fibres as a cause of brain damage due to head injury: A pathological study of twenty cases. *The Lancet,* **278**: pp. 443-448.

Tartaglia, M. C., Hazrati, L., Davis, K. D., Green, R. E. A., Wennberg, R., Mikulis, D., et al. (2014). Chronic traumatic encephalopathy and other neurodegenerative proteinopathies. *Frontiers in Human Neuroscience,* **8**: p.30.

Tator, C. (2009). Concussions are brain injuries and should be taken seriously. *The Canadian Journal of Neurological Sciences.* **36**(3): p. 269.

Thibault, L.E., Gennarelli, T.A., Margulies, S.S., Marcus, J., and Eppinger, R. The strain dependent pathophysiological consequences of inertial loading on central nervous system tissue, *Proc. IRCOBI Conf*., 1990, Lyon, France, pp.191-202.

Thomas, L.M., Roberts, V.L., Gurdjian, E.S. (1966). Experimental intracranial pressure gradients in the human skull. *Journal of Neurology, Neurosurgery & Psychiatry*, **29**: pp. 404–411.

Thomas, L. M., Roberts, V. L., & Gurdjian, E. S. (1967). Impact-induced pressure gradients along three orthogonal axes in the human skull. *Journal of Neurosurgery,* **26**(3): p. 316.

Viano, D. C., King, A. I., Melvin, J. W., & Weber, K. (1989). Injury biomechanics research: An essential element in the prevention of trauma. *Journal of Biomechanics,* **22**(5): pp. 403-417.

Walsh, E.S. & Hoshizaki, T.B. Comparative analysis of the Hybrid III neckform to unbiased neckforms using a centric and non-centric impact protocol. ASTM Symposium on the mechanism of concussion in sports, 2012, Atlanta, GA, November 13th.

Walsh, E., Post, A. et al. (2012). Dynamic impact response characteristics of a helmeted hybrid III headform using a centric and non- centric impact protocol. Proceedings of the Institution of Mechanical Engineers, Part P: Journal of Sports Engineering and Technology, **226**(3-4): pp.220–25.

Walsh, E., Rousseau, P., & Hoshizaki, T. (2011). The influence of impact location and angle on the dynamic impact response of a hybrid III headform. *Sports Engineering,* **13**(3): pp. 135-143.

Wennberg, R. and Tator, C. (2003). National hockey league reported concussions, 1986-87 to 2001-02. Canadian Journal of Neurological Sciences, **30**(3): pp.206–9.

Willinger, R. & Baumgarthner, D. (2003). Human head tolerance limit to specific injury mechanisms. *International Journal of Crashworthiness*, **8**(6): pp. 605-617.

Willinger, R., Ryan, G. A., McLean, A. J. & Kopp, C. M. Mechanisms of brain injury related to mathematical modeling and epidemiological data, *Proceedings of the International IRCOBI Conference on the Biomechanics of Impacts*, 1992, pp. 179-192.

Willinger, R., Taleb, L. & Kopp, C. (1995). Modal and temporal analysis of head mathematical models. *Journal Neurotrauma*, **12**: pp.743–54.

Xiong, Y., Mahmood, A., & Chopp, M. (2013). Animal models of traumatic brain injury. *Nature Reviews Neuroscience*, **14**(2): p. 128.

Yoganandan, N., Pintar, F. A., Zhang, J., & Baisden, J. L. (2009). Physical properties of the human head: Mass, center of gravity and moment of inertia. *Journal of Biomechanics,* **42**(9): pp. 1177-1192.

Yogandandan N, Li J, Zhang J, et al. (2008). Influence of angular acceleration-deceleration pulse shapes on regional brain strains. *Journal of Biomechanics* **41**: pp. 2253–2262.

Zhang, L., Yang, K. H., King, A. I. (2004). A proposed injury threshold for mild traumatic brain injury. Journal of Biomechanical Engineering, **126**: pp.226–36.

Zhang, L., Yang, K. H., & King, A. I. (2001). Biomechanics of neurotrauma. *Neurological Research,* **23**(2-3): p. 144.

Zhou, C., Khalil, T.B. & King, A.I. A New Model Comparing Impact Responses of the homogeneous and Inhomogeneous Human Brain. *39th Stapp Car Crash Conference*, 1995, Coronado CA, SAE International, Warrendale, PA.

Appendix 1

Research Design

Table 5: Experimental design for low compliance striker.

C1	A1	A2	A3
B1	C1A1B1	C1A2B1	C1A3B1
B2	C1A1B2	C1A2B2	C1A3B2
B3	C1A1B3	C1A2B3	C1A3B3
B4	C1A1B4	C1A2B4	C1A3B4
B5	C1A1B5	C1A2B5	C1A3B5

Table 6: Experimental design for medium compliance striker.

C2	A1	A2	A3
B1	C2A1B1	C2A2B1	C2A3B1
B2	C2A1B2	C2A2B2	C2A3B2
B3	C2A1B3	C2A2B3	C2A3B3
B4	C2A1B4	C2A2B4	C2A3B4
B5	C2A1B5	C2A2B5	C2A3B5

Table 7: Experimental design for high compliance striker.

C3	A1	A2	A3
B1	C3A1B1	C3A2B1	C3A3B1
B2	C3A1B2	C3A2B2	C3A3B2
B3	C3A1B3	C3A2B3	C3A3B3
B4	C3A1B4	C3A2B4	C3A3B4
B5	C3A1B5	C3A2B5	C3A3B5

Legend:

Velocity:

A1: Velocity 1 (4.5m/s)

A2: Velocity 2 (6m/s)

A3: Velocity 3 (7.5m/s)

Location:

B1: Site 1

B2: Site 2

B3: Site 3

B4: Site 4

B5: Site 5

Compliance:

C1: Compliance 1 (5-7ms)

C2: Compliance 2 (12-15ms)

C3: Compliance 3(20+ms)